Biogeosciences
Discussions
Open Access
EGU

Functional convergence of biosphere–atmosphere interactions in response to meteorology

Christopher Krich[1,2], Mirco Migliavacca[1], Diego G. Miralles[2], Guido Kraemer[1,3], Tarek S. El-Madany[1], Markus Reichstein[1], Jakob Runge[4], and Miguel D. Mahecha[3]

[1]Max Planck Institute for Biogeochemistry, 07745 Jena,Germany
[2]Hydro-Climate Extremes Lab (H-CEL), Faculty of Bioscience Engineering, Ghent University, Ghent, Belgium
[3]Remote Sensing Centre for Earth System Research, Leipzig University, 04103, Leipzig, Germany
[4]German Aerospace Center, Institute of Data Science, 07745, Jena, Germany

Correspondence: Christopher Krich (ckrich@bgc-jena.mpg.de)

Abstract. Understanding the dependencies of the terrestrial carbon and water cycle is a prerequisite to anticipate their behaviour under climate change conditions. However, terrestrial ecosystems and the atmosphere interact via a multitude of variables, time- and space scales. Additionally the interactions might differ among vegetation types or climatic regions. Today, novel algorithms aim to disentangle the causal structure behind such interaction from empirical data. Visualising the esti-

5   mated structure in networks, the nodes represent relevant meteorological determinants and land-surface fluxes, and the links dependencies among them possibly including their lag and strength. Here we show that biosphere–atmosphere interactions are strongly shaped by meteorological conditions. For example, we find that temperate and high latitude ecosystems during peak productivity exhibit very similar biosphere–atmosphere interaction networks as tropical forests. In times of anomalous conditions like drought though, both ecosystems behave more like Mediterranean ecosystems during their dry season. Our

10   results demonstrate that ecosystems from different climate or vegetation types have similar biosphere–atmosphere interactions if their meteorological conditions are similar. We anticipate our analysis to foster the use of network approaches as they allow a more comprehensive understanding of the state of ecosystem functioning. Long term or even irreversible changes in network structure are rare and thus can be indicators of fundamental functional ecosystem shifts.

1 Introduction

15   Ecosystems and the atmosphere constantly exchange energy, matter, and momentum (Bonan, 2015). These interactions result in biosphere–atmosphere fluxes (in particular carbon, water and sensible heat fluxes) that are shaped by a variety of climatic conditions and states of the terrestrial biosphere (McPherson, 2007). Understanding how biosphere–atmosphere fluxes interact and how they causally depend on the short-term meteorological and long-term climate conditions is crucial for building predictive terrestrial biosphere models (Detto et al., 2012; Green et al., 2017). However, the exact causal structure of dependencies

20   between surface and atmosphere variables is still subject to unknowns (Baldocchi et al., 2016; Miralles et al., 2019). For example, we still do not understand well under which conditions certain climate extremes turn ecosystems into carbon sources or sinks (Sippel et al., 2017; Flach et al., 2018; von Buttlar et al., 2018). One reason for our incomplete understanding is that the

causal dependencies underlying biosphere–atmosphere interactions might vary among ecosystems due to their structure and
long-term adaptation to climatic conditions. An other is that causal techniques are still rarely used. The collection of global
25 long-term observation of biosphere–atmosphere fluxes measured via the eddy covariance method in FLUXNET (Baldocchi,
2014) should, however, allow us to disentangle such questions.

A variety of causal discovery methods have been developed over the past few years (see Runge et al., 2019a, for a recent
overview). They allow to infer causal networks from empirical data enabled by certain general assumptions about the under-
lying processes. Some methods only consider two variables, such as (bivariate classical) Granger causality (Granger, 1969),
30 convergent cross mapping (Sugihara et al., 2012), or transfer entropy (Schreiber, 2000). Other methods allow us to understand
how multiple variables interact, accounting for common drivers and mediators by using conditioning approaches as suggested
by multiple studies (Detto et al., 2012; Goodwell and Kumar, 2017; Papagiannopoulou et al., 2017; Claessen et al., 2019;
Runge et al., 2019b). One example for the latter is PCMCI, a combination of the PC algorithm (named after its inventors Peter
and Clark (Spirtes and Glymour, 1991)) and the Momentary Conditional Independence (MCI) test (Runge et al., 2019b). Krich
35 et al. (2020) showed that the PCMCI approach is useful to assess causal dependencies of ecosystem fluxes and atmospheric
variables.

In this study, we use multivariate time series from global ecological observation networks such as FLUXNET to investigate
how biosphere–atmosphere interactions vary across vegetation types and climate zones. If biosphere–atmosphere interactions
substantially vary across climate gradients or among vegetation types, then this may indicate that responses to climatic extremes
40 may differ substantially and require terrestrial biosphere models to account for them differently. If, however, the opposite
applies and ecosystems of the Earth exhibit similar biosphere–atmosphere interaction types, then common principles can be
identified that can serve as empirical reference for global vegetation models. The assessment of these questions includes
investigating the effect of extreme meteorological events on the network structure of biosphere–atmosphere interactions.

To do so, we characterise biosphere–atmosphere interactions as weighted networks estimated via PCMCI (see Sect. 2.3). The
45 nodes in these networks represent biosphere–atmosphere fluxes and meteorological variables (see Sect. 2.1). Any significant
dependence among the variables is depicted as a link between the respective nodes and the link strength is measured by the MCI
partial correlation value (see Sect. 2.2). We estimated overall 10.038 networks from 119 ecosystems using sliding windows
of three months over the available time-series length. This captures also an ecosystem's temporal development. Each of the
estimated networks constitutes one high-dimensional observation with a network's links spanning the high dimensional space.
50 Projecting this high dimensional space onto two dimensions using methods of non-linear dimensionality reduction (here t-
SNE, see Sect. 2.4) reveals the dominant features of transitions between different states of biosphere–atmosphere interactions,
i.e., which links are strong descriptors of differences between networks. We then start with analysing the structure of the low
dimensional embedding (Sect. 3.1). Subsequently we focus on ecosystem level behaviour, i.e. the seasonal median (Sect. 3.3)
and individual years during extreme conditions (Sect. 3.4). Section 3.5 puts the results into broader perspective.

2 Data and Methods

2.1 Eddy-covariance observations

We used eddy covariance data from the FLUXNET database (Baldocchi et al., 2001) aggregated to daily time resolution. To maximise the available ecosystems and time series length, we took the union of the LaThuile Fair use (Baldocchi, 2008) and FLUXNET2015 Tier 1 (Pastorello et al., 2020) datasets (Nelson et al.) with at least 5 years of measurement. If a site year was available in both datasets we selected the one from FLUXNET2015. A detailed list of used sites and years is given in table A1. The final dataset contains sites from the major plant functional types and covers the major Koeppen-Geiger climate classes, i.e. tropical to polar climate zones. The majority of sites belong to evergreen needleleaf forests, grasslands and deciduous broadleaf forests. The dominant climate classes are continental, temperate and dry climates. The dataset's variables, including meteorological and eddy covariance measurements, were quality checked, filtered, gap-filled, and partitioned with standard tools (Papale et al., 2006; Pastorello et al., 2020) and provided with per-variable quality flags. We extracted following variables, comparable between the two dataset, and their corresponding quality controls (if available): shortwave downward radiation (or global radiation, R_g), air temperature (T), net ecosystem exchange (NEE) (positive values signify carbon uptake into the biosphere), vapour pressure deficit (VPD), sensible heat- (H), latent heat flux (LE), gross primary productivity (GPP), precipitation (P) and soil water content (SWC, measured at the shallowest sensor). Within the FLUXNET2015 dataset these variables are named as: "SW_IN_F_MDS", "TA_F_MDS", "NEE_VUT_USTAR50", "VPD_F_MDS", "H_F_MDS", "LE_F_MDS", "GPP_NT_VUT_USTAR50", "P", "SWC_F_MDS_1", respectively. Correspondingly for the LaThuile dataset:"Rg_f", "Tair_f", "NEE_f", "VPD_f", "LE_f", "H_f", "GPP_f", "precip", "SWC1_f", respectively. GPP is calculated via the commonly used night time flux partitioning (Reichstein et al., 2005). Here GPP is the difference between NEE and ecosystem respiration. The latter is estimated via a model which is parameterized using night time values of NEE.

2.2 PCMCI

To analyse biosphere–atmosphere interactions, we estimated network structures using the causal network discovery algorithm PCMCI. PCMCI is tailored to estimate time-lagged dependencies from potentially high-dimensional and autocorrelated multivariate time series. Dependencies can be interpreted causally under certain assumptions. The algorithm is explained from a biogeoscience viewpoint in Krich et al. (2020). A comprehensive description from theoretical assumptions to numerical experiments is given in Runge et al. (2019b).

As a brief summary, PCMCI efficiently conducts conditional independence tests among the contemporaneous (i.e. the dependence between two non-lagged variables) and time-lagged (up to some maximum time lag) variables to reconstruct a dependency network. While PCMCI can also be combined with nonlinear tests, here we estimate conditional independence using partial correlation (ParCorr), implying that we only consider linear dependencies. Partial correlation between X and Y given Z is defined as the correlation between the residuals of X and Y after regressing out the (potentially multivariate) condition Z.

PCMCI has two phases. In the first phase, the 'condition selection', a superset of lagged parents of each variable is estimated based on a fast variant of the PC algorithm (Spirtes and Glymour, 1991). In the second phase 'momentary conditional independence' (MCI) among all pairs of contemporaneous and lagged variables $(X_{t-\tau}^i, X_t^j)$ for $\tau \geq 0$ is estimated. The MCI

90   test removes the influence of the lagged drivers (obtained in the first phase) and yields p-values (based on a two-sided t-test) for causal links among each time-lagged and contemporaneous variable pair. The strength of links is here given by the MCI partial correlation. Lagged links are directed forward in time and contemporaneous dependencies are left undirected. A causal interpretation of links rests on the standard assumptions of causal discovery (Runge et al., 2019b). In particular, a statistical independence (here at a 0.1 two-sided significance level) between a pair of variables conditional on the other lagged variables

95   is interpreted as the absence of a causal link (Faithfulness condition). On the other hand, a causal interpretation of the estimated links is here to be understood only with respect to the variables included in the analysis. Unobserved common drivers can still render links as spurious. In the present context we aim to classify networks and a causal interpretation of each link is not the focus. The dependence structure among variables can finally be visualised by weighted networks with link weights given by the MCI partial correlation. MCI partial correlation removes the influence of other lagged drivers and autocorrelation, yielding

100   a better interpretation of the strength of a causal mechanism than the common Pearson correlation. At the same time, MCI partial correlation values are normalised in [-1, 1] and can, hence, well be compared between variable pairs with different units of measurement.

2.3   Network Estimation

Networks are estimated using PCMCI between the variables R_g, T, NEE, VPD, H and LE using time lags between zero

105   to five days (see Supplementary Material Table B1 for settings). Based on findings in Krich et al. (2020), we subtracted a smoothed seasonal mean from each variable to remove the common driver influence of the seasonal cycle that would yield spurious dependencies. The seasonal mean was smoothed by setting the high frequency components (> 20 days$^-$) of its Fourier transform to zero. We estimated networks in sliding windows of three months, taking the centre month as the time index of each network. To avoid effects on the network structure from gap-filling we used the following quality flag thresholds.

110   A daily datapoint is not used if its quality flag is below 0.6 (i.e. more than 60% of measured and good quality gap filled data). In case more than 25% of datapoints of the three month window are flagged as bad quality, the time window is removed from the analysis. To analyse the factors influencing network structure, we consider the mean values over the respective time period of the variables included in the network calculation, and additionally those of GPP, P and SWC. GPP, P and SWC were not included in the network calculation because certain characteristics can impinge on network estimation. GPP is derived using

115   NEE and T. Any of the links GPP–T and GPP–NEE thus could be due to its processing rather than an actual dependence. P, on the other hand, typically yields non intuitive results due to its binary character (precipitation - no precipitation).

2.4   Dimensionality Reduction

Applying above described procedure we obtained 10.038 networks for the different months and sites. Each network, with 6 variables and 6 time lags, contains 216 links and can, hence, be embedded into a 216 dimensional space. However, here we only

120 focus on the 15 contemporaneous links since we found them to be strongest and most robust. Therefore, the dimensionality
reduction step was performed on those links only. For the dimensionality reduction, we tested principal component analysis
(PCA; Pearson, 1901), t-distributed stochastic neighbour embedding (t-SNE; Maaten and Hinton, 2008), and uniform mani-
fold approximation and projection (UMAP; McInnes et al., 2018). PCA is the standard method for dimensionality reduction,
it is commonly used, linear, fast, and easily interpretable regarding the meaning of its axes (the principal components). A PCA

125 embedding typically fails to reveal complex clusterings, because it maintains large scale gradients but often produces embed-
dings in which far away points appear very close in the embedding. In contrast t-SNE preserves local neighbourhoods which
makes it very good at visualising clusters in the data and non-linear relationships. Drawbacks are the difficult interpretability of
the embedding axes due to the non-linear nature and its fairly long computation time for large datasets. UMAP was developed
as an improvement of t-SNE regarding computation time while having an embedding with similar properties as t-SNE.

130 As we are dealing with an unsupervised method there is no obvious measure to assess the quality of an embedding, as each
method optimises a different error function. A measure commonly used for the comparison and characterisation of dimension-
ality methods is the agreement between K-ary neighborhoods (the K nearest points to an observation) in the high dimensional
and low dimensional space. The measure $R_{\mathrm{NX}}(K)$ (Lee et al., 2015) gives a measure of the improvement of the embedding of
K-ary neighborhoods over random embeddings. For an embedding with random coordinates we obtain $R_{\mathrm{NX}}(K) \approx 0$ and if the

135 K-ary neighborhoods are perfectly preserved we obtain $R_{\mathrm{NX}}(K) = 1$. As this measure depends on the neighborhood size, K,
we can draw a curve over K that characterizes if the method is better at maintaining global or local neighborhoods. The area
under the $R_{\mathrm{NX}}(K)$ curve gives an idea of the overall quality of the embedding. An intercomparison of the three dimensionality
reduction methods using this measure shows t-SNE to perform best (see Fig. A1, B1, C1).

2.5 Clustering and median network trajectories

140 On the reduced space we applied a clustering method named Ordering Points To Identify the Clustering Structure (OPTICS;
Ankerst et al., 1999). Clusters are found by identifying regions of high density that contain a certain number of datapoints. The
cluster borders are defined by a certain drop in reachability of further datapoints. This allows points that lie outside the reacha-
bility of neighbouring clusters to remain unclustered. Following settings were used for clustering: $\mathrm{min_{samples}}{=}80$, $\mathrm{max_{eps}}{=}8$ and
xi=0.5. We calculated mean networks for each cluster by calculating the mean MCI value for each contemporaneous link of

145 each network contained in the cluster and only took those links that had an absolute value above 0.2. Further, for each ecosys-
tem, we calculated an annual median trajectory within the t-SNE space which is composed of its monthly median networks. To
this end, we calculated non-intercepting convex hulls which consisted of at least three datapoints (networks within the t-SNE
space belonging to the same ecosystem, representing the same month, in at least three years). The monthly median network is
the average of the networks lying on (≥ 3 networks) or in the inner hull (< 3 networks).

Biogeosciences
Discussions

Open Access

EGU

3   Results and Discussions

3.1   Two-dimensional embedding of biosphere–atmosphere networks

The dimensionality reduction method t-SNE performed best at projecting the high dimensional space created by the networks contemporaneous links onto two dimensions (cf. Sect. 2.4, Fig. A1, B1). The two-dimensional embedding of biosphere–atmosphere interactions is ordered primarily by dependencies including carbon flux (NEE) and energy distributions (LE, H). This can be seen in Fig. 1 which shows the embedding colour coded by the strength of individual links, i.e. MCI partial correlation values. The colouring reveals that the link strengths are ordered along gradients. The strongest gradients measured via distance correlations (Székely et al., 2007) are given by the links NEE–LE ($\rho = 0.75$), Rg–LE ($\rho = 0.73$) and T–H ($\rho = 0.69$). The connection between carbon and water fluxes as well as the role of energy input to sustain water fluxes are well known and investigated dependencies (Beer et al., 2010; Luyssaert et al., 2007). Further, gradients of mean climatic conditions emerge. This is depicted in Fig. 2 showing again the low dimensional embedding, this time colour coded by the networks' underlying mean conditions, i.e. the average over the respective time window, of the exchange rates (GPP, NEE, LE and H) as well as meteorological conditions (Rg, T, VPD, P). Clearly, the mean exchange rates and meteorological conditions - although not considered in the estimation of the networks - are related to the observed biosphere–atmosphere interactions. On the contrary, corresponding vegetation types and Köppen-Geiger classes are not much related as displayed in the Supplementary Material section Fig. D2. The results show that a high dimensional space encompassing more than 10000 ecosystem networks representing the states of biosphere–atmosphere interactions from ecosystems of various geographic origins can be reduced to a compact two dimensional manifold characterised by four edges and gradients of biosphere and atmosphere conditions. While gradients in MCI partial correlation strength are expected as they were used as features in the dimensionality reduction, gradients in climatic and biospheric conditions were not. This information thus must be entailed in the networks' structure. To better grasp the distribution of network structures, we further analyse the emerging clusters.

3.2   Clusters of characteristic ecosystem–atmosphere networks

As we apply a significance threshold to each link of the estimated network structures (see Sect. 2.3), the networks typically lack weak links. This leads to a certain degree of clustering among the networks, which we identified using the OPTICS approach (see Sect. 2.5; Ankerst et al., 1999)) (Fig. 3a). Cluster boundaries are shown by the convex hulls in Fig. 3b, where we also visualise the mean interaction networks of each cluster. Based on this analysis we can identify four archetypes of network structures:

Type 1 is a sparsely connected network. Links, if present, are very weak and predominantly exist among atmospheric variables. Mean atmospheric conditions are characterised by low energy input (low R_g and T). Carbon and water fluxes are consequently close to zero, and daily averages of sensible heat can even reach negative values. Such conditions reflect high latitude ecosystem winter states experienced by ecosystems like the evergreen needle leave forests (ENF) of Finnland,
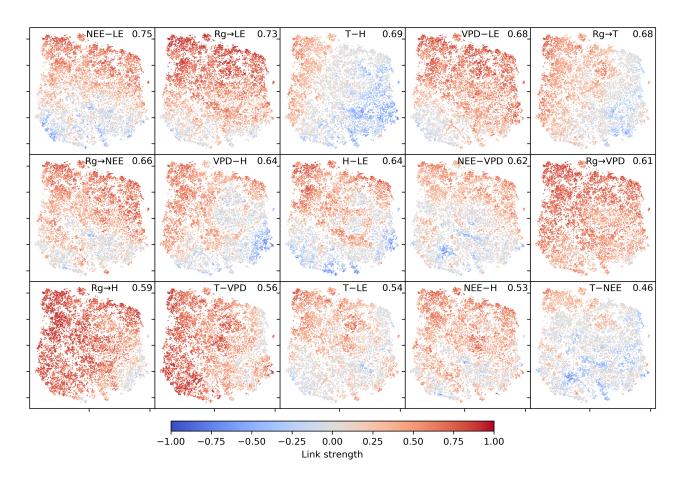
Figure 1. Two-dimensional embedding of three-monthly biosphere–atmosphere networks realised via t-SNE. Shown is the distribution of link strengths among the networks. The strength is estimated via MCI partial correlation values. Subfigures are sorted by the distance correlation of the link's MCI value with the axes (value in upper right corner). As R_g can only be a cause, connections including R_g are directed →.

i.e. Hyytiälä (FI-Hyy) and Sodankyla (FI-Sod) as well as Canada, i.e., the UCI-1850 burn site (CA-NS1) and Quebec - Eastern Boreal (CA-Qcu) during December and January.

Type 2 consists of strong links among atmospheric variables but LE and NEE are weakly, not, or even negatively connected. This network structure coincides with high energy input (high R_g and T) but low water availability (low P and SWC, high VPD). A high Bowen ratio, i.e. the ratio between sensible heat and latent heat, representing aridity, and low carbon fluxes are the consequence. These conditions are typically present at semi-arid ecosystems like the woody savanna (WSA) Santa Rita Mesquite (US-SRM) as well as the grasslands Santa Rita (US-SRG), Audubon Research Ranch (US-Aud) and Sturt Plains (AU-Stp) during dry season.
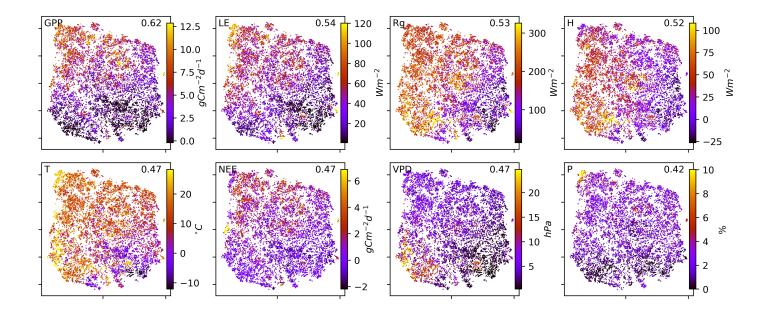
185

Figure 2. Two-dimensional embedding coloured by underlying mean exchange rates and meteorological conditions. The mean values are calculated over the respective time periods used for the network estimation. Each network is estimated on a three month window of daily time series data. Values are cut off at the highest and lowest percentile.

Type 3 exhibits the same strong links among Rg, VPD and H as Type 2 but T is weakly or not connected and the opposite for LE and NEE. R_g and T are considerably lower than in Type 2 but because of sufficient water availability the Bowen ratio is between 0 and 1. Typical ecosystems in this state are mid to high latitude forests during spring or autumn, e.g. Harvard Forest EMS Tower (US-Ha1, deciduous broadleaf forest (DBF)), Roccarespampani 1 (IT-Ro1, DBF), Vielsalm (BE-Vie, mixed forest (MF)) and Hyytiälä (FI-Hyy, ENF).

Type 4 is fully and strongly connected. Both energy input and water availability are high leading to Bowen ratios around 1. This network state is typically present in tropical forests like the Guyaflux site in French Guiana (GF-Guy) (evergreen broadleaf forest (EBF)) but can temporarily be also reached by a variety of other ecosystems, e.g. mid and high latitude forests like Hainich (DE-Hai, DBF), Tharandt (DE-Tha, ENF), BE-Vie (MF), FI-Hyy (ENF) as well as woody savannas (WSA) as Howard Springs (AU-How) and grasslands as Daly River Savanna (AU-Dap).

The archetypes of networks are located at the edges of the two-dimensional space and thus could define two imaginary axes. From a physical point of view, energy is required for each process and interaction to occur, e.g. photosynthesis or evaporation (Bonan, 2015). Therefore, transitions along the axis connecting the network types 1 and 4 might be interpreted as energy
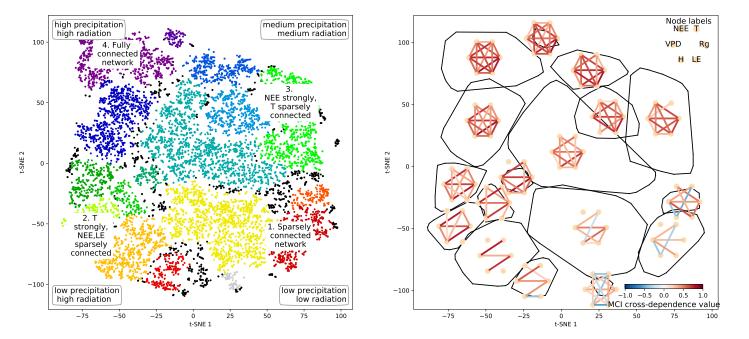
Figure 3. Structure of the two-dimensional embedding. left: t-SNE space clustered by the OPTICS approach (Ankerst et al., 1999). Colours represent different clusters, black dots are not attributed to a cluster. Indicated are the four archetypes of network connectivity and the networks underlying meteorological conditions. right: Convex hulls of clusters and their average network, i.e. average over all networks belonging to one cluster. Average networks are thresholded at a minimum link strength of 0.2. A finer clustering can be found in the Supplementary Material section Fig. D1.

controlled as dependencies among all variables fade or increase consistently. Transitions along the axis connecting network types 2 and 3 are explainable by a combination of water availability and a temperature gradient. Low water availability but high temperatures lead to low carbon and water fluxes and thus low connectivity. On the other hand sufficient water and

205   medium temperatures allow for fluxes but likely reduce the influence of varying temperatures leading to connected NEE and LE but disconnected T. And indeed these patterns and gradients exist. Mean R_g is lowest at network type 1 and almost linearly increases towards network type 4. P is lowest at network type 1 and 2. In combination with high energy input network type 2 has lowest SWC values and the highest Bowen ratios (see Supplementary Material section Fig. D2). SWC is higher but quite dispersed elsewhere suggesting that at a certain point water limitations are fading out. T values of course also show an increase

210   from network type 1 to 4 (as radiation) but also from network type 3 to 2 and are actually rather low (8°C to 15 °C) at network type 3 (see Fig 2). As meteorological conditions affect biosphere productivity, network type 1 and 2 exhibit low, type 3 medium and type 4 high productivity i.e. estimated as GPP. In short, the clustering revealed that changes in energy and water availability can explain major transitions between different states of biosphere–atmosphere interactions. Having an understanding of the low dimensional embedding's structure now allows us to analyse specific ecosystem behaviour.

3.3 Ecosystems' median trajectories

Each point in the reduced t-SNE space represents a biosphere–atmosphere interaction network for a given month and ecosystem. Hence, we can trace an ecosystem's trajectory through time. An ecosystem's median annual trajectory (see Sect. 2.5) within the low dimensional space reflects seasonal patterns of meteorological conditions (Fig. 4). For example, mid-latitude sites like FR-Pue (EBF), DE-Hai (DBF) and FI-Hyy (ENF) exhibit a strong seasonal variation of R_g and span a long distance in the t-SNE space. In contrast, tropical ecosystems like GF-Guy (EBF) constantly have high R_g and exhibit predominantly network type 4 indicative of high productive conditions - while DE-Hai or FI-Hyy reach this connectivity pattern only during peak growing season. US-SRM (WSA), however, has similar or even higher R_g values throughout the year but barely manages to deviate from type 2 which is in accordance with its low water availability. The amount of precipitation further aligns with differences and characteristics of the trajectories of FR-Pue, DE-Hai and FI-Hyy. For example, FI-Hyy shows some deviation towards edge 2 in February and March, FR-Pue in June, July and August. For both, mean precipitation is lowest during these month. The strong control by energy and water availability is in line with a recent analysis showing that variability in land-surface processes is largely explained by productivity measures as well as water and energy availability. Both, water and energy availability, need to be high for high productive states, yet the lack of either of them leads to low productivity (Kraemer et al., 2020). This biosphere state triangle is found in our analysis by the network type 1 (cold), 2 (dry) and 4 (high productivity). Yet, a fourth network type (type 3) is naturally occurring in the t-SNE space as we here include interactions with the atmosphere.

3.4 Deviations from ecosystem median trajectories

Climatic extremes are visible in an ecosystem's trajectory as strong deviations from the median trajectory. Figure 5 shows the trajectories of ecosystems during anomalous dry or wet conditions. During the European heatwave of 2003, in July and August the trajectories of two temperate central European forests, DE-Hai and DE-Tha, no longer manage to establish a network structure resembling network type 4, typical for these ecosystems during their high productive phase. Instead they are shifted towards network type 2, associated with drier conditions (Fig. 5a, b). Similarly, the ecosystem BR-Sa3 (EBF) in the Brazilian tropical rainforest shows substantial deviations towards network type 2 during the exceptional dry season of 2001 (Aug, Sep, Oct) (Marengo et al., 2018) (Fig. 5c). In contrast, US-Wkg is a grassland accustomed to dry conditions and thus predominantly exhibits low water and carbon fluxes resulting in network structures as of network type 2, i.e. water and carbon fluxes are barely or even disconnected. Carbon and water fluxes of semi-arid ecosystems, however, are known to respond quickly and strongly to sufficient precipitation (Potts et al., 2019; Leon et al., 2014; Reynolds et al., 2004). This sensitivity is found to carry over to the network structure as well. The network structure of US-Wkg becomes fully connected (network type 4) in September 2014 with above average precipitation (NOAA) (Fig. 5d). The relevance of climatic conditions in controlling biosphere–atmosphere interactions on three monthly time windows thus shows also on ecosystem level as they are strong enough to explain deviations from an ecosystem's median trajectory and lead to the detection of climatic extremes.
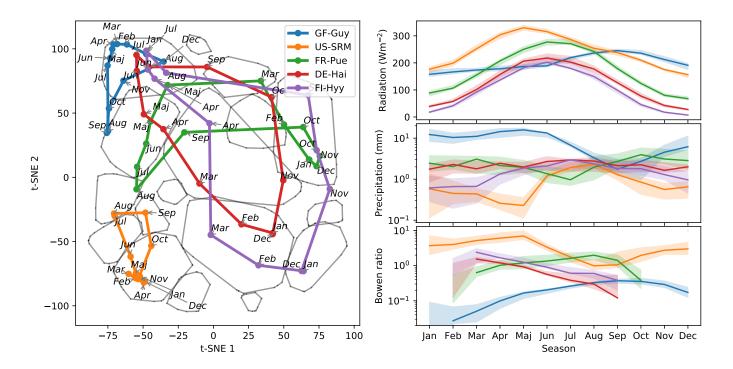
Figure 4. Median trajectories of selected sites (left) and their corresponding mean values of radiation, precipitation and the Bowen ratio (right). As networks are calculated using a centred three month moving window, each month is ascribed a network. Thus, the behaviour of an ecosystem can be tracked by its monthly networks, which form trajectories for each year. An ecosystem's median trajectory is composed of the two dimensional monthly median networks (see Sect. 2.5 for details).

3.5 Functional convergence of biosphere–atmosphere interactions

We have seen that networks representing biosphere–atmosphere interactions are strongly shaped by prevailing mean meteorological conditions. Moreover, the visualisation of ecosystem trajectories within the t-SNE space (Fig. 4, 5) and the distributions of vegetation types and climatic regions (Supplementary Material Fig. D2) reveal that ecosystems across vegetation types and climatic regions can exhibit similar biosphere–atmosphere interactions if their meteorological conditions are similar. For example, at high radiation and water availability, i.e. optimal growing conditions, ecosystems exhibit fully connected networks (type 4) as well as high carbon and water fluxes. Diverging from optimal growing conditions, links in the networks weaken and disappear. This behaviour can be understood as functional convergence of ecosystems which corroborates the hypothesis that ecosystems have a low number of key processes that determine ecosystem behaviour (Lambert, 2006; Meinzer, 2003; Shaver et al., 2007) rendering their behaviour transparent and predictable. Criticism might rise as the larger part of the biosphere–atmosphere interaction network indeed is a pure atmospheric network, i.e. Rg, T, VPD and H. Thus strong associations of networks and their trajectories with atmospheric conditions could be dominated by changes in this atmospheric network. Fig.
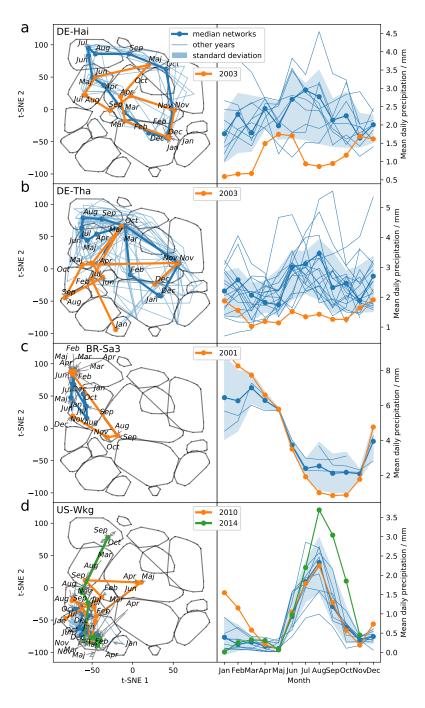
Figure 5. Abnormal conditions in meteorological conditions (here precipitation) become visible in an ecosystem's trajectory. left: Trajectories within the low dimensional space of the ecosystems Hainich (DE-Hai, DBF), Tharand (DE-Tha, ENF), Santarem-Km83-Logged Forest (BR-Sa3, EBF) and Walnut Gulch Kendall Grasslands (US-Wkg, GRA). right: Three monthly average of daily precipitation data.
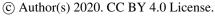
1, however, suggests the opposite. The strongest gradients are given by the links NEE–LE and Rg–LE and transitions along the axis connecting type 2 and 3 (cf. Fig. 3) are dominated by changes in biosphere connectivity, i.e. LE and NEE.

260   In fact, the dominance of climatic drivers in controlling the temporal evolution of ecosystem functioning emerges also in other studies (Musavi et al., 2017; Schwalm et al., 2017) as they showed that carbon fluxes are primarily controlled by climatic factors. Yet, these and others also show the role of biotic factors in shaping the responses of ecosystem processes to climatic variability. For example, Musavi et al. (2017) revealed in a global ecosystem study that species diversity and ecosystem age decrease inter annual variability of GPP. Similarly, Wagg et al. (2017) discovered biodiversity to increase long-term stability

265 of ecosystem productivity. In regional studies Wales et al. (2020) found the stability of net primary production to be affected by the kind and severity of disturbances. Tamrakar et al. (2018) showed that seasonal carbon fluxes were more sensitive to environmental conditions in a homogeneous forest compared to a heterogeneous one. It would be of interest to investigate, to which degree the effects of biotic factors also translates to the sensitivity of the network structure.

    Furthermore, extreme heat and drought events (Sippel et al., 2018) or compound events in general (Zscheischler et al., 2020)

270 can severely disrupt ecosystem functions. The time of recovery from such disturbances is a crucial parameter in assessing ecosystem resilience. Schwalm et al. (2017) showed that the recovery time measured as the recovery in GPP is primarily influenced by climate but secondarily by biodiversity and CO_2 fertilisation. Assessing the recovery time via GPP already puts the ecosystem functioning into focus. The here presented framework, i.e. the sensitivity of an ecosystem's network structure to meteorological conditions, might be a valuable asset to study reaction time and strength to and recovery from extreme events as

275 it not only utilises one variable but the interactions of a set of variables, thereby capturing more comprehensively an ecosystem state. A drawback is the reduced temporal resolution (a certain time period of daily or even half hourly measurements is aggregated to one network) which can be offset by the here used moving window approach to a certain degree. Especially with regard to climatic extreme conditions in recent years with observed vegetation dieback in, for example, DE-Hai (Schuldt et al., 2020), further studies could also shed light on the role of adaptation in shaping biosphere–atmosphere interactions. Our study

280 suggest that adaptation to a lesser degree limits the range of possible interactions but enables to sustain and persist certain conditions for longer periods. The focus of further studies thus could be to elucidate the role of biotic factors in influencing ecosystem trajectories as well as the role of adaptation and the response to extreme events.

4   Conclusions

We analysed the functional behaviour of a variety of ecosystems using the FLUXNET database of eddy covariance measure-

285 ments. In particular, we examined the interaction structure between biosphere–atmosphere fluxes as well as atmospheric state variables using PCMCI, an algorithm to estimate causal relationships from empirical time series. In total we included 119 measurement sites with cumulative 1067 measurement years leading to 10038 monthly networks. Using non-linear dimensionality reduction, we found four archetypes of network states defining the edges of the low dimensional embedding. They are characterised on the one hand by a fully connected and almost unconnected network structure and on the other hand by an

290 antagonistic coupling of carbon and water flux with temperature - when one is strongly coupled, the other is decoupled. The

transitions between these states correlate well with gradients of meteorological drivers, i.e. radiation and water availability. The movement of an ecosystem within that space therefore strongly aligns with changes in meteorological conditions. This, however, also leads to similar behaviour under similar conditions for strongly contrasting ecosystems. For example, forests of mid or even high latitudes exhibit similar interaction structure as tropical forests given high radiation and water availability

295 during summer. Yet, this state can also be reached by predominantly dry ecosystems like steppe grasslands given sufficient precipitation. In contrast if productive ecosystems are struck by a severe drought, like central European ecosystems in 2003, the behaviour can adapt more to that of a Mediterranean ecosystem. Overall this analysis shows that the biosphere-atmosphere interaction structure can adapt flexibly to prevailing conditions and is widely independent of vegetation type and climatic region. Such behaviour is strong evidence for functional convergence of ecosystems, i.e. their behaviour is determined by a low

300 number of key processes. For further studies, we suggest, to focus on the role of biotic factors as, for example, plant functional types, ecosystem age and adaptation. These factors could play crucial roles in copying strategies of climatic extremes.

Code availability. Code scripts can be found at https://github.com/ckrich/Functional-convergence-of-biosphere-atmosphere-interactions-in-response-to-meteorology

Data availability. The eddy covariance data of the FLUXNET sites can be downloaded from the official webpage (https://fluxnet.fluxdata.org/).

305 **Appendix A: Methods**

Table A1: List of FLUXNET sites used for the generation of artificial datasets and the time period used.

FLUXNET-ID	start year	end year	data reference	FLUXNET-ID	start year	end year	data reference
AT-Neu	2002	2012	Wohlfahrt et al. (2008)	IT-BCi	2004	2014	Vitale et al. (2016)
AU-ASM	2010	2014	Cleverly et al. (2013)	IT-Col	1996	2014	Valentini et al. (1996)
AU-Cpr	2010	2014	Meyer et al. (2015)	IT-Cpz	1997	2009	Garbulsky et al. (2008)
AU-DaP	2007	2013	Beringer et al. (2011a)	IT-Lav	2003	2014	Marcolla et al. (2003)
AU-DaS	2008	2014	Hutley et al. (2011)	IT-MBo	2003	2013	Marcolla et al. (2011)
AU-Dry	2008	2014	Cernusak et al. (2011)	IT-Noe	2004	2014	Reichstein et al. (2002)
AU-How	2001	2014	Beringer et al. (2007)	IT-Non	2001	2006	Nardino et al. (2002)
AU-Stp	2008	2014	Beringer et al. (2011b)	IT-Ren	1998	2013	Marcolla et al. (2005)
AU-Tum	2001	2014	Leuning et al. (2005)	IT-Ro1	2000	2008	Rey et al. (2002)
AU-Wom	2010	2014	Arndt et al.	IT-Ro2	2002	2012	Tedeschi et al. (2006)
BE-Bra	1996	2014	Carrara et al. (2004)	IT-SRo	1999	2012	Chiesi et al. (2005)

Continued on next page

Table A1 – *Continued from previous page*

FLUXNET-ID	start year	end year	data reference	FLUXNET-ID	start year	end year	data reference
BE-Lon	2004	2014	Moureaux et al. (2006)	IT-Tor	2008	2014	Galvagno et al. (2013)
BE-Vie	1996	2014	Aubinet et al. (2001)	JP-SMF	2002	2006	Matsumoto et al. (2008)
BR-Sa3	2000	2004	Saleska et al. (2003)	NL-Hor	2004	2011	Jacobs et al. (2007)
CA-Mer	1998	2005	Lafleur et al. (2003)	NL-Loo	1996	2014	Moors (2012)
CA-NS1	2001	2005	Goulden et al. (2006)	PT-Esp	2002	2006	Rodrigues et al. (2011)
CA-NS2	2001	2005	Bond-Lamberty et al. (2004)	RU-Cok	2003	2014	van der Molen et al. (2007)
CA-NS3	2001	2005	Wang et al. (2002a)	RU-Fyo	1998	2014	Kurbatova et al. (2008)
CA-NS5	2001	2005	Wang et al. (2002b)	SD-Dem	2005	2009	Ardö et al. (2008)
CA-NS6	2001	2005	Wang et al. (2002c)	SE-Deg	2001	2005	Sagerfors et al. (2008)
CA-Qcu	2001	2006	Giasson et al. (2006)	SE-Fla	1996	2002	Valentini et al. (2000)
CA-Qfo	2003	2010	Chen et al. (2006)	SE-Nor	1996	2005	Lagergren et al. (2008)
CA-SF2	2001	2005	Rayment and Jarvis (1999a)	UK-Gri	1997	2006	Medlyn et al. (2005)
CA-SF3	2001	2006	Rayment and Jarvis (1999b)	US-ARM	2003	2012	Fischer et al. (2007)
CH-Cha	2005	2014	Merbold et al. (2014)	US-Aud	2002	2006	-
CH-Dav	1997	2014	Zielis et al. (2014)	US-Blo	1997	2007	Schade et al.
CH-Fru	2005	2014	Imer et al. (2013)	US-Bo1	1996	2007	Meyers and Hollinger (2004)
CH-Lae	2004	2014	Etzold et al. (2011)	US-Cop	2001	2007	Ruehr et al. (2012a)
CH-Oe1	2002	2008	Ammann et al. (2009)	US-FPe	2000	2006	Gilmanov et al. (2005)
CH-Oe2	2004	2014	Dietiker et al. (2010)	US-GBT	1999	2006	Zeller and Hehn (1996)
CZ-BK1	2004	2014	Acosta et al. (2013)	US-GLE	2004	2014	Zeller and Nikolov (2000)
CZ-BK2	2004	2012	-	US-Ha1	1991	2012	Wofsy et al. (1993)
CZ-wet	2006	2014	Dušek et al. (2012)	US-Ho1	1996	2004	Armstrong and Ernst (1999)
DE-Akm	2009	2014	-	US-Los	2000	2014	Baker et al. (2003)
DE-Geb	2001	2014	Anthoni et al. (2004b)	US-MMS	1999	2014	Pryor et al. (1999)
DE-Gri	2004	2014	Prescher et al. (2010a)	US-Me2	2002	2014	McDowell et al. (2004)
DE-Hai	2000	2012	Knohl et al. (2003)	US-Me6	2010	2014	Ruehr et al. (2012b)
DE-Kli	2004	2014	Prescher et al. (2010b)	US-Myb	2010	2014	Ruehr et al. (2012c)
DE-Lkb	2009	2013	Lindauer et al. (2014)	US-NR1	1998	2014	Reich et al. (1998)
DE-Obe	2008	2014	-	US-Ne1	2001	2013	Gitelson et al. (2003)
DE-Spw	2010	2014	-	US-Ne2	2001	2013	Cassman et al. (2003a)
DE-Tha	1996	2014	Grünwald and Bernhofer (2007)	US-Ne3	2001	2013	Cassman et al. (2003b)
DE-Wet	2002	2006	Anthoni et al. (2004a)	US-PFa	1995	2014	Yi et al. (2001)

Continued on next page

Table A1 – *Continued from previous page*

FLUXNET-ID	start year	end year	data reference	FLUXNET-ID	start year	end year	data reference
DK-NuF	2008	2014	Westergaard-Nielsen et al. (2013)	US-Prr	2010	2014	Ruehr et al. (2012d)
DK-Sor	1996	2014	Pilegaard et al. (2011)	US-SP1	2000	2005	Thomas et al. (1999a)
DK-ZaH	2000	2014	Lund et al. (2012)	US-SP2	1998	2004	Thomas et al. (1999b)
ES-ES1	1999	2006	Sanz et al. (2004)	US-SP3	1999	2004	Thomas et al. (1999c)
FI-Hyy	1996	2014	Suni et al. (2003)	US-SRG	2008	2014	Ruehr et al. (2012e)
FI-Kaa	2000	2006	Aurela et al. (2007)	US-SRM	2004	2014	Scott et al. (2008)
FI-Sod	2001	2014	Thum et al. (2007)	US-Syv	2001	2014	Desai et al. (2005)
FR-Fon	2005	2014	Delpierre et al. (2016)	US-Ton	2001	2014	Tang et al. (2003)
FR-Gri	2004	2014	Loubet et al. (2011)	US-Twt	2009	2014	Hatala et al. (2012)
FR-Hes	1997	2006	Granier et al. (2000)	US-UMB	2000	2014	Rothstein et al. (2000)
FR-LBr	1996	2008	Berbigier et al. (2001)	US-UMd	2007	2014	Nave et al. (2011)
FR-Pue	2000	2014	Rambal et al. (2004)	US-Var	2000	2014	Xu et al. (2004)
GF-Guy	2004	2014	Bonal et al. (2008)	US-WCr	1999	2014	Potter et al. (2001)
HU-Bug	2002	2006	Nagy et al. (2005)	US-Whs	2007	2014	Scott et al. (2006)
IL-Yat	2001	2006	Grünzweig et al. (2003)	US-Wkg	2004	2014	Emmerich (2003)
IT-Amp	2002	2006	Gilmanov et al. (2007)	ZA-Kru	2000	2013	Archibald et al. (2009)
IT-BCi	2004	2014	Vitale et al. (2016)	ZM-Mon	2000	2009	Merbold et al. (2009)

Table B1. PCMCI parameters that were used differently from default settings.

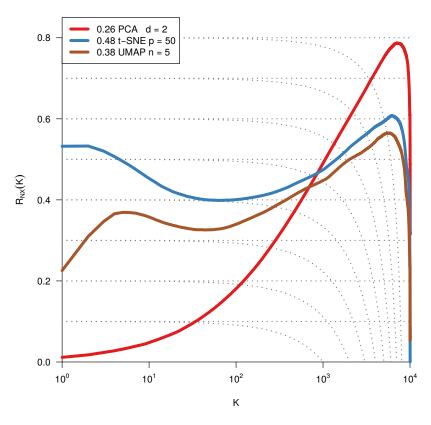| PCMCI parameter	Setting
significance α	0.1
α_{pc}	None
tau_min	0
tau_max	5
selected_variables	T, NEE, VPD, H, LE
mask_type	'y'
fdr_method	'fdr_bh'

Figure A1. Quality assessment of dimensionality reduction techniques. To visualize and subsequently analyse the network space we reduce its dimensionality. We compared PCA, t-SNE and UMAP including various parameter settings (here: PCA's leading two principal components, t-SNE with perplexity 30, and UMAP with $n_{neighbors}$ equal 5 for 2 dimensions). The test statistic $R_{NX}(k)$ (y-axis) gives the improvement of the embedding of k-neighborhoods (x-axis) over a random embedding. The area under the curves (preserving the log-scaled x-axis) is given in the legend and gives an idea of the overall quality of the embedding Lee et al. (2015). We chose t-SNE with perplexity 30, as it preserves best local neighbourhoods and performs well on larger distances.

Appendix C: Results and Discussion

Figure B1. Same metric as Fig. A1. Optimisation of the dimensionality reduction via t-SNE by using different perplexity values.
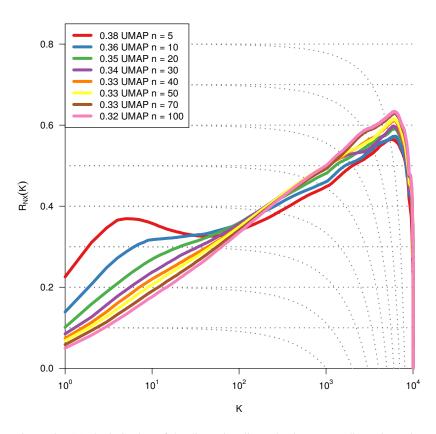
Figure C1. Same metric as Fig. A1. Optimisation of the dimensionality reduction to two dimensions via UMAP by using different values for the parameter $n_{neighbors}$.
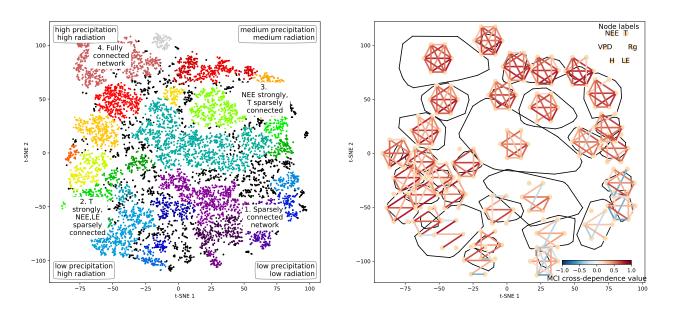
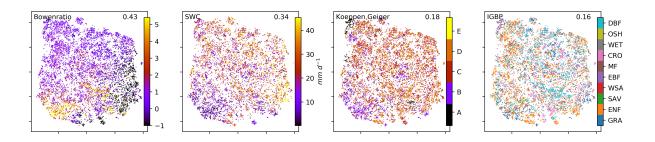**Figure D1.** As Fig. 3 but with smaller clusters exhibiting the finer structure of the t-SNE space.

Figure D2. t-SNE space coloured by underlying mean Bowenratio and precipitation, as well as the ecosystems respective Koeppen Geiger class and IGBP type.
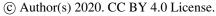
Author contributions. CK and MDM designed the study with contributions from all other authors. CK conducted the analysis and wrote the manuscript. All authors helped to improve the manuscript.

Competing interests. The authors declare that they have no competing financial interests.

References

Acosta, M., Pavelka, M., Montagnani, L., Kutsch, W., Lindroth, A., Juszczak, R., and Janouš, D.: Soil Surface CO2 Efflux Measurements in Norway Spruce Forests: Comparison between Four Different Sites across Europe — from Boreal to Alpine Forest, Geoderma, 192, 320   295–303, https://doi.org/10.1016/j.geoderma.2012.08.027, 2013.

Ammann, C., Spirig, C., Leifeld, J., and Neftel, A.: Assessment of the Nitrogen and Carbon Budget of Two Managed Temperate Grassland Fields, Agriculture, Ecosystems & Environment, 133, 150–162, https://doi.org/10.1016/j.agee.2009.05.006, 2009.

Ankerst, M., Breunig, M. M., Kriegel, H.-P., and Sander, J.: OPTICS: ordering points to identify the clustering structure, ACM Sigmod record, 28, 49–60, 1999.

325   Anthoni, P., Knohl, A., Rebmann, C., Freibauer, A., Mund, M., Ziegler, W., Kolle, O., and Schulze, E.-D.: Forest and agricultural land-use-dependent CO2 exchange in Thuringia, Germany, Global Change Biology, 10, 2005–2019, 2004a.

Anthoni, P. M., Knohl, A., Rebmann, C., Freibauer, A., Mund, M., Ziegler, W., Kolle, O., and Schulze, E.-D.: Forest and Agricultural Land-Use-Dependent CO2 Exchange in Thuringia, Germany, Global Change Biology, 10, 2005–2019, https://doi.org/10.1111/j.1365-2486.2004.00863.x, 2004b.

330   Archibald, S. A., Kirton, A., van der Merwe, M. R., Scholes, R. J., Williams, C. A., and Hanan, N.: Drivers of Inter-Annual Variability in Net Ecosystem Exchange in a Semi-Arid Savanna Ecosystem, South Africa, Biogeosciences, 6, 251–266, https://doi.org/https://doi.org/10.5194/bg-6-251-2009, 2009.

Ardö, J., Mölder, M., El-Tahir, B. A., and Elkhidir, H. A. M.: Seasonal Variation of Carbon Fluxes in a Sparse Savanna in Semi Arid Sudan, Carbon Balance and Management, 3, 7, https://doi.org/10.1186/1750-0680-3-7, 2008.

335   Armstrong, N. and Ernst, E.: The treatment of eczema with Chinese herbs: a systematic review of randomized clinical trials, British journal of clinical pharmacology, 48, 262, 1999.

Arndt, S., Hinko-Najera, N., Griebel, A., Beringer, J., and Livesley, S. J.: FLUXNET2015 AU-Wom Wombat, https://doi.org/10.18140/FLX/1440207.

Aubinet, M., Chermanne, B., Vandenhaute, M., Longdoz, B., Yernaux, M., and Laitat, E.: Long Term Carbon Dioxide Exchange above a 340   Mixed Forest in the Belgian Ardennes, Agricultural and Forest Meteorology, 108, 293–315, https://doi.org/https://doi.org/10.1016/S0168-1923(01)00244-1, 2001.

Aurela, M., Riutta, T., Laurila, T., Tuovinen, J.-P., Vesala, T., Tuittila, E.-S., Rinne, J., Haapanala, S., and Laine, J.: CO2 exchange of a sedge fen in southern Finland-The impact of a drought period, Tellus B: Chemical and Physical Meteorology, 59, 826–837, 2007.

Baker, I., Denning, A. S., Hanan, N., Prihodko, L., Uliasz, M., Vidale, P.-L., Davis, K., and Bakwin, P.: Simulated and Observed 345   Fluxes of Sensible and Latent Heat and CO2 at the WLEF-TV Tower Using SiB2.5, Global Change Biology, 9, 1262–1277, https://doi.org/10.1046/j.1365-2486.2003.00671.x, 2003.

Baldocchi, D.: 'Breathing' of the terrestrial biosphere: lessons learned from a global network of carbon dioxide flux measurement systems, Australian Journal of Botany, 56, 1–26, 2008.

Baldocchi, D.: Measuring fluxes of trace gases and energy between ecosystems and the atmosphere – the state and future of the eddy covari-350   ance method, Global Change Biology, 20, 3600–3609, https://doi.org/10.1111/gcb.12649, http://dx.doi.org/10.1111/gcb.12649, 2014.

Baldocchi, D., Falge, E., Gu, L., Olson, R., Hollinger, D., Running, S., Anthoni, P., Bernhofer, C., Davis, K., Evans, R., Fuentes, J., Gold-stein, A., Katul, G., Law, B., Lee, X., Malhi, Y., Meyers, T., Munger, W., Oechel, W., Paw U, K. T., Pilegaard, K., Schmid, H. P., Valentini, R., Verma, S., Vesala, T., Wilson, K., and Wofsy, S.: FLUXNET: A New Tool to Study the Temporal and Spatial Vari-

ability of Ecosystem-Scale Carbon Dioxide, Water Vapor, and Energy Flux Densities, Bulletin of the American Meteorological Society, 82, 2415–2434, https://doi.org/10.1175/1520-0477(2001)082<2415:FANTTS>2.3.CO;2, https://doi.org/10.1175/1520-0477(2001)082<2415:FANTTS>2.3.CO;2, 2001.

Baldocchi, D., Ryu, Y., and Keenan, T.: Terrestrial Carbon Cycle Variability [version 1; peer review: 2 approved, F1000Research, 5(F1000 Faculty Rev), https://doi.org/(https://doi.org/10.12688/f1000research.8962.1), 2016.

Beer, C., Reichstein, M., Tomelleri, E., Ciais, P., Jung, M., Carvalhais, N., Rödenbeck, C., Arain, M. A., Baldocchi, D., Bonan, G. B., Bondeau, A., Cescatti, A., Lasslop, G., Lindroth, A., Lomas, M., Luyssaert, S., Margolis, H., Oleson, K. W., Roupsard, O., Veenendaal, E., Viovy, N., Williams, C., Woodward, F. I., and Papale, D.: Terrestrial Gross Carbon Dioxide Uptake: Global Distribution and Covariation with Climate, Science, 329, 834–838, https://doi.org/10.1126/science.1184984, http://science.sciencemag.org/content/329/5993/834, 2010.

Berbigier, P., Bonnefond, J.-M., and Mellmann, P.: CO2 and Water Vapour Fluxes for 2 Years above Euroflux Forest Site, Agricultural and Forest Meteorology, 108, 183–197, https://doi.org/10.1016/S0168-1923(01)00240-4, 2001.

Beringer, J., Hutley, L. B., Tapper, N. J., and Cernusak, L. A.: Savanna Fires and Their Impact on Net Ecosystem Productivity in North Australia, Global Change Biology, 13, {990–1004}, https://doi.org/{10.1111/j.1365-2486.2007.01334.x}, 2007.

Beringer, J., Hutley, L. B., Hacker, J. M., Neininger, B., and U, K. T. P.: Patterns and Processes of Carbon, Water and Energy Cycles across Northern Australian Landscapes: From Point to Region, Agricultural and Forest Meteorology, 151, {1409–1416}, https://doi.org/{10.1016/j.agrformet.2011.05.003}, 2011a.

Beringer, J., Hutley, L. B., Hacker, J. M., Neininger, B., and U, K. T. P.: Patterns and Processes of Carbon, Water and Energy Cycles across Northern Australian Landscapes: From Point to Region, Agricultural and Forest Meteorology, 151, 1409–1416, https://doi.org/https://doi.org/10.1016/j.agrformet.2011.05.003, savanna Patterns of Energy and Carbon Integrated Across the Landscape (SPECIAL), 2011b.

Bonal, D., Bosc, A., Ponton, S., Goret, J.-Y., Burban, B., Gross, P., Bonnefond, J.-M., Elbers, J., Longdoz, B., Epron, D., Guehl, J.-M., and Granier, A.: Impact of Severe Dry Season on Net Ecosystem Exchange in the Neotropical Rainforest of French Guiana, Global Change Biology, 14, 1917–1933, https://doi.org/10.1111/j.1365-2486.2008.01610.x, 2008.

Bonan, G.: Ecological Climatology: Concepts and Applications, Cambridge University Press, 3 edn., https://doi.org/10.1017/CBO9781107339200, 2015.

Bond-Lamberty, B., Wang, C., and Gower, S. T.: Net Primary Production and Net Ecosystem Production of a Boreal Black Spruce Wildfire Chronosequence, Global Change Biology, 10, 473–487, https://doi.org/10.1111/j.1529-8817.2003.0742.x, 2004.

Carrara, A., Janssens, I. A., Yuste, J. C., and Ceulemans, R.: Seasonal Changes in Photosynthesis, Respiration and NEE of a Mixed Temperate Forest, Agricultural and Forest Meteorology, 126, 15–31, https://doi.org/https://doi.org/10.1016/j.agrformet.2004.05.002, 2004.

Cassman, K. G., Dobermann, A., Walters, D. T., and Yang, H.: Meeting Cereal Demand While Protecting Natural Resources and Improving Environmental Quality, Annual Review of Environment and Resources, 28, 315–358, https://doi.org/10.1146/annurev.energy.28.040202.122858, 2003a.

Cassman, K. G., Dobermann, A., Walters, D. T., and Yang, H.: Meeting Cereal Demand While Protecting Natural Resources and Improving Environmental Quality, Annual Review of Environment and Resources, 28, 315–358, https://doi.org/10.1146/annurev.energy.28.040202.122858, 2003b.

390 Cernusak, L. A., Hutley, L. B., Beringer, J., Holtum, J. A. M., and Turner, B. L.: Photosynthetic Physiology of Eucalypts along a Sub-Continental Rainfall Gradient in Northern Australia, Agricultural and Forest Meteorology, 151, {1462–1470}, https://doi.org/{10.1016/j.agrformet.2011.01.006}, 2011.

Chen, J. M., Govind, A., Sonnentag, O., Zhang, Y., Barr, A., and Amiro, B.: Leaf Area Index Measurements at Fluxnet-Canada Forest Sites, Agricultural and Forest Meteorology, 140, 257–268, https://doi.org/10.1016/j.agrformet.2006.08.005, 2006.

395 Chiesi, M., Maselli, F., Bindi, M., Fibbi, L., Cherubini, P., Arlotta, E., Tirone, G., Matteucci, G., and Seufert, G.: Modelling Carbon Budget of Mediterranean Forests Using Ground and Remote Sensing Measurements, Agricultural and Forest Meteorology, 135, 22–34, https://doi.org/10.1016/j.agrformet.2005.09.011, 2005.

Claessen, J., Molini, A., Martens, B., Detto, M., Demuzere, M., and Miralles, D.: Global biosphere–climate interaction: a multi-scale appraisal of observations and models, Biogeosciences Discussions, 2019, 1–30, https://doi.org/10.5194/bg-2019-212, https://www.
400 biogeosciences-discuss.net/bg-2019-212/, 2019.

Cleverly, J., Boulain, N., Villalobos-Vega, R., Grant, N., Faux, R., Wood, C., Cook, P. G., Yu, Q., Leigh, A., and Eamus, D.: Dynamics of Component Carbon Fluxes in a Semi-Arid Acacia Woodland, Central Australia, Journal of Geophysical Research: Biogeosciences, 118, {1168–1185}, https://doi.org/{10.1002/jgrg.20101}, 2013.

Delpierre, N., Berveiller, D., Granda, E., and Dufrêne, E.: Wood Phenology, Not Carbon Input, Controls the Interannual Variability of Wood
405 Growth in a Temperate Oak Forest, New Phytologist, 210, 459–470, https://doi.org/10.1111/nph.13771, 2016.

Desai, A. R., Bolstad, P. V., Cook, B. D., Davis, K. J., and Carey, E. V.: Comparing Net Ecosystem Exchange of Carbon Dioxide between an Old-Growth and Mature Forest in the Upper Midwest, USA, Agricultural and Forest Meteorology, 128, 33–55, https://doi.org/10.1016/j.agrformet.2004.09.005, 2005.

Detto, M., Molini, A., Katul, G., Stoy, P., Palmroth, S., and Baldocchi, D.: Causality and Persistence in Ecological Systems: A Nonparametric
410 Spectral Granger Causality Approach., The American Naturalist, 179, 524–535, https://doi.org/10.1086/664628, https://doi.org/10.1086/664628, pMID: 22437181, 2012.

Dietiker, D., Buchmann, N., and Eugster, W.: Testing the Ability of the DNDC Model to Predict CO2 and Water Vapour Fluxes of a Swiss Cropland Site, Agriculture, Ecosystems & Environment, 139, 396–401, https://doi.org/10.1016/j.agee.2010.09.002, 2010.

Dušek, J., Čížková, H., Stellner, S., Czerný, R., and Květ, J.: Fluctuating Water Table Affects Gross Ecosystem Production and Gross
415 Radiation Use Efficiency in a Sedge-Grass Marsh, Hydrobiologia, 692, 57–66, https://doi.org/10.1007/s10750-012-0998-z, 2012.

Emmerich, W. E.: Carbon Dioxide Fluxes in a Semiarid Environment with High Carbonate Soils, Agricultural and Forest Meteorology, 116, 91–102, https://doi.org/10.1016/S0168-1923(02)00231-9, 2003.

Etzold, S., Ruehr, N. K., Zweifel, R., Dobbertin, M., Zingg, A., Pluess, P., Häsler, R., Eugster, W., and Buchmann, N.: The Carbon Balance of Two Contrasting Mountain Forest Ecosystems in Switzerland: Similar Annual Trends, but Seasonal Differences, Ecosystems, 14, 1289–
420 1309, https://doi.org/10.1007/s10021-011-9481-3, 2011.

Fischer, M. L., Billesbach, D. P., Berry, J. A., Riley, W. J., and Torn, M. S.: Spatiotemporal Variations in Growing Season Exchanges of CO2, H2O, and Sensible Heat in Agricultural Fields of the Southern Great Plains, Earth Interactions, 11, 1–21, https://doi.org/10.1175/EI231.1, 2007.

Flach, M., Sippel, S., Gans, F., Bastos, A., Brenning, A., Reichstein, M., and Mahecha, M. D.: Contrasting biosphere responses to hydromete-
425 orological extremes: revisiting the 2010 western Russian heatwave, Biogeosciences, 15, 6067–6085, https://doi.org/10.5194/bg-15-6067-2018, https://www.biogeosciences.net/15/6067/2018/, 2018.

Galvagno, M., Wohlfahrt, G., Cremonese, E., Rossini, M., Colombo, R., Filippa, G., Julitta, T., Manca, G., Siniscalco, C., di Cella, U. M., and Migliavacca, M.: Phenology and Carbon Dioxide Source/Sink Strength of a Subalpine Grassland in Response to an Exceptionally Short Snow Season, Environmental Research Letters, 8, 025 008, https://doi.org/10.1088/1748-9326/8/2/025008, 2013.

430 Garbulsky, M. F., Peñuelas, J., Papale, D., and Filella, I.: Remote Estimation of Carbon Dioxide Uptake by a Mediterranean Forest, Global Change Biology, 14, 2860–2867, https://doi.org/10.1111/j.1365-2486.2008.01684.x, 2008.

Giasson, M.-A., Coursolle, C., and Margolis, H. A.: Ecosystem-level CO2 fluxes from a boreal cutover in eastern Canada before and after scarification, Agricultural and Forest Meteorology, 140, 23–40, 2006.

Gilmanov, T., Soussana, J.-F., Aires, L., Allard, V., Ammann, C., Balzarolo, M., Barcza, Z., Bernhofer, C., Campbell, C., Cernusca, A.,
435   et al.: Partitioning European grassland net ecosystem CO2 exchange into gross primary productivity and ecosystem respiration using light response function analysis, Agriculture, ecosystems & environment, 121, 93–120, 2007.

Gilmanov, T. G., Tieszen, L. L., Wylie, B. K., Flanagan, L. B., Frank, A. B., Haferkamp, M. R., Meyers, T. P., and Morgan, J. A.: Integration of CO2 flux and remotely-sensed data for primary production and ecosystem respiration analyses in the Northern Great Plains: Potential for quantitative spatial extrapolation, Global Ecology and Biogeography, 14, 271–292, 2005.

440 Gitelson, A. A., Viña, A., Arkebauer, T. J., Rundquist, D. C., Keydan, G., and Leavitt, B.: Remote Estimation of Leaf Area Index and Green Leaf Biomass in Maize Canopies, Geophysical Research Letters, 30, https://doi.org/10.1029/2002GL016450, 2003.

Goodwell, A. E. and Kumar, P.: Temporal Information Partitioning Networks (TIPNets): A process network approach to infer ecohydrologic shifts, Water Resources Research, 53, 5899–5919, https://doi.org/10.1002/2016WR020218, https://agupubs.onlinelibrary.wiley.com/doi/abs/10.1002/2016WR020218, 2017.

445 Goulden, M. L., Winston, G. C., McMILLAN, A. M. S., Litvak, M. E., Read, E. L., Rocha, A. V., and Elliot, J. R.: An Eddy Covariance Mesonet to Measure the Effect of Forest Age on Land–Atmosphere Exchange, Global Change Biology, 12, 2146–2162, https://doi.org/10.1111/j.1365-2486.2006.01251.x, 2006.

Granger, C. W. J.: Investigating Causal Relations by Econometric Models and Cross-spectral Methods, Econometrica, 37, 424–438, http://www.jstor.org/stable/1912791, 1969.

450 Granier, A., Ceschia, E., Damesin, C., Dufrêne, E., Epron, D., Gross, P., Lebaube, S., Le Dantec, V., Le Goff, N., Lemoine, D., et al.: The carbon balance of a young beech forest, Functional ecology, 14, 312–325, 2000.

Green, J., G. Konings, A., Alemohammad, S. H., Berry, J., Entekhabi, D., Kolassa, J., Lee, J.-E., and Gentine, P.: Regionally strong feedbacks between the atmosphere and terrestrial biosphere, NATURE GEOSCIENCE, 10, 410–414, https://doi.org/http://dx.doi.org/10.1038/ngeo2957, https://www.nature.com/ngeo/journal/v10/n6/pdf/ngeo2957.pdf, 2017.

455 Grünwald, T. and Bernhofer, C.: A Decade of Carbon, Water and Energy Flux Measurements of an Old Spruce Forest at the Anchor Station Tharandt, Tellus B: Chemical and Physical Meteorology, 59, 387–396, https://doi.org/10.1111/j.1600-0889.2007.00259.x, 2007.

Grünzweig, J., Lin, T., Rotenberg, E., Schwartz, A., and Yakir, D.: Carbon sequestration in arid-land forest, Global Change Biology, 9, 791–799, 2003.

Hatala, J. A., Detto, M., and Baldocchi, D. D.: Gross Ecosystem Photosynthesis Causes a Diurnal Pattern in Methane Emission from Rice,
460   Geophysical Research Letters, 39, https://doi.org/10.1029/2012GL051303, 2012.

Hutley, L. B., Beringer, J., Isaac, P. R., Hacker, J. M., and Cernusak, L. A.: A Sub-Continental Scale Living Laboratory: Spatial Patterns of Savanna Vegetation over a Rainfall Gradient in Northern Australia, Agricultural and Forest Meteorology, 151, {1417–1428}, https://doi.org/{10.1016/j.agrformet.2011.03.002}, 2011.

Imer, D., Merbold, L., Eugster, W., and Buchmann, N.: Temporal and Spatial Variations of Soil CO_2, CH_4 and N_2O Fluxes at Three Differently

465   Managed Grasslands, Biogeosciences, 10, 5931–5945, https://doi.org/https://doi.org/10.5194/bg-10-5931-2013, 2013.

Jacobs, C. M. J., Jacobs, A. F. G., Bosveld, F. C., Hendriks, D. M. D., Hensen, A., Kroon, P. S., Moors, E. J., Nol, L., Schrier-
        Uijl, A., and Veenendaal, E. M.: Variability of Annual CO_2 Exchange from Dutch Grasslands, Biogeosciences, 4, 803–816,
        https://doi.org/https://doi.org/10.5194/bg-4-803-2007, 2007.

Knohl, A., Schulze, E.-D., Kolle, O., and Buchmann, N.: Large Carbon Uptake by an Unmanaged 250-Year-Old Deciduous Forest in Central

470   Germany, Agricultural and Forest Meteorology, 118, 151–167, https://doi.org/10.1016/S0168-1923(03)00115-1, 2003.

Kraemer, G., Camps-Valls, G., Reichstein, M., and Mahecha, M. D.: Summarizing the state of the terrestrial biosphere in few dimensions,
        Biogeosciences, 17, 2397–2424, 2020.

Krich, C., Runge, J., Miralles, D. G., Migliavacca, M., Perez-Priego, O., El-Madany, T., Carrara, A., and Mahecha, M. D.: Estimating causal
        networks in biosphere–atmosphere interaction with the PCMCI approach, Biogeosciences, 17, 1033–1061, https://doi.org/10.5194/bg-17-

475   1033-2020, https://www.biogeosciences.net/17/1033/2020/, 2020.

Kurbatova, J., Li, C., Varlagin, A., Xiao, X., and Vygodskaya, N.: Modeling Carbon Dynamics in Two Adjacent Spruce Forests with Different
        Soil Conditions in Russia, Biogeosciences, 5, 969–980, https://doi.org/https://doi.org/10.5194/bg-5-969-2008, 2008.

Lafleur, P. M., Roulet, N. T., Bubier, J. L., Frolking, S., and Moore, T. R.: Interannual variability in the peatland-atmosphere carbon dioxide
        exchange at an ombrotrophic bog, Global Biogeochemical Cycles, 17, 2003.

480 Lagergren, F., Lindroth, A., Dellwik, E., Ibrom, A., Lankreijer, H., Launiainen, S., Mölder, M., Kolari, P., Pilegaard, K., and Vesala, T.:
        Biophysical controls on CO2 fluxes of three Northern forests based on long-term eddy covariance data, Tellus B: Chemical and Physical
        Meteorology, 60, 143–152, 2008.

Lambert, W. D.: Functional convergence of ecosystems: evidence from body mass distributions of North American late Miocene mammal
        faunas, Ecosystems, 9, 97–118, 2006.

485 Lee, J. A., Peluffo-Ordóñez, D. H., and Verleysen, M.: Multi-Scale Similarities in Stochastic Neighbour Embedding: Reducing Dimension-
        ality While Preserving Both Local and Global Structure, Neurocomputing, 169, 246–261, https://doi.org/10.1016/j.neucom.2014.12.095,
        2015.

Leon, E., Vargas, R., Bullock, S., Lopez, E., Panosso, A. R., and La Scala, N.: Hot spots, hot moments, and spatio-
        temporal controls on soil CO2 efflux in a water-limited ecosystem, Soil Biology and Biochemistry, 77, 12 – 21,

490   https://doi.org/https://doi.org/10.1016/j.soilbio.2014.05.029,   http://www.sciencedirect.com/science/article/pii/S0038071714002004,
        2014.

Leuning, R., Cleugh, H. A., Zegelin, S. J., and Hughes, D.: Carbon and Water Fluxes over a Temperate Eucalyptus Forest and a Tropical
        Wet/Dry Savanna in Australia: Measurements and Comparison with MODIS Remote Sensing Estimates, Agricultural and Forest Meteo-
        rology, 129, 151–173, https://doi.org/https://doi.org/10.1016/j.agrformet.2004.12.004, 2005.

495 Lindauer, M., Schmid, H. P., Grote, R., Mauder, M., Steinbrecher, R., and Wolpert, B.: Net Ecosystem Exchange over a Non-Cleared
        Wind-Throw-Disturbed Upland Spruce Forest—Measurements and Simulations, Agricultural and Forest Meteorology, 197, 219–234,
        https://doi.org/10.1016/j.agrformet.2014.07.005, 2014.

Loubet, B., Laville, P., Lehuger, S., Larmanou, E., Fléchard, C., Mascher, N., Genermont, S., Roche, R., Ferrara, R. M., Stella, P., Personne,
        E., Durand, B., Decuq, C., Flura, D., Masson, S., Fanucci, O., Rampon, J.-N., Siemens, J., Kindler, R., Gabrielle, B., Schrumpf, M., and

500   Cellier, P.: Carbon, Nitrogen and Greenhouse Gases Budgets over a Four Years Crop Rotation in Northern France, Plant and Soil, 343,
        109, https://doi.org/10.1007/s11104-011-0751-9, 2011.

Lund, M., Falk, J. M., Friborg, T., Mbufong, H. N., Sigsgaard, C., Soegaard, H., and Tamstorf, M. P.: Trends in CO2 Exchange in a High Arctic Tundra Heath, 2000–2010, Journal of Geophysical Research: Biogeosciences, 117, https://doi.org/10.1029/2011JG001901, 2012.

Luyssaert, S., Inglima, I., Jung, M., Richardson, A. D., Reichstein, M., Papale, D., Piao, S., Schulze, E.-D., Wingate, L., Matteucci, G., et al.: CO2 balance of boreal, temperate, and tropical forests derived from a global database, Global change biology, 13, 2509–2537, 2007.

Maaten, L. v. d. and Hinton, G.: Visualizing data using t-SNE, Journal of machine learning research, 9, 2579–2605, 2008.

Marcolla, B., Pitacco, A., and Cescatti, A.: Canopy Architecture and Turbulence Structure in a Coniferous Forest, Boundary-Layer Meteorology, 108, 39–59, https://doi.org/10.1023/A:1023027709805, 2003.

Marcolla, B., Cescatti, A., Montagnani, L., Manca, G., Kerschbaumer, G., and Minerbi, S.: Importance of advection in the atmospheric CO2 exchanges of an alpine forest, Agricultural and Forest Meteorology, 130, 193–206, 2005.

Marcolla, B., Cescatti, A., Manca, G., Zorer, R., Cavagna, M., Fiora, A., Gianelle, D., Rodeghiero, M., Sottocornola, M., and Zampedri, R.: Climatic Controls and Ecosystem Responses Drive the Inter-Annual Variability of the Net Ecosystem Exchange of an Alpine Meadow, Agricultural and Forest Meteorology, 151, 1233–1243, https://doi.org/10.1016/j.agrformet.2011.04.015, 2011.

Marengo, J. A., Alves, L. M., Alvala, R., Cunha, A. P., Brito, S., and Moraes, O. L.: Climatic characteristics of the 2010-2016 drought in the semiarid Northeast Brazil region, Anais da Academia Brasileira de Ciências, 90, 1973–1985, 2018.

Matsumoto, K., Ohta, T., Nakai, T., Kuwada, T., Daikoku, K., Iida, S., Yabuki, H., Kononov, A. V., van der Molen, M. K., Kodama, Y., Maximov, T. C., Dolman, A. J., and Hattori, S.: Energy Consumption and Evapotranspiration at Several Boreal and Temperate Forests in the Far East, Agricultural and Forest Meteorology, 148, 1978–1989, https://doi.org/10.1016/j.agrformet.2008.09.008, 2008.

McDowell, N. G., Bowling, D. R., Bond, B. J., Irvine, J., Law, B. E., Anthoni, P., and Ehleringer, J. R.: Response of the Carbon Isotopic Content of Ecosystem, Leaf, and Soil Respiration to Meteorological and Physiological Driving Factors in a Pinus Ponderosa Ecosystem, Global Biogeochemical Cycles, 18, https://doi.org/10.1029/2003GB002049, 2004.

McInnes, L., Healy, J., and Melville, J.: UMAP: Uniform Manifold Approximation and Projection for Dimension Reduction, 2018.

McPherson, R. A.: A review of vegetation—atmosphere interactions and their influences on mesoscale phenomena, Progress in Physical Geography, 31, 261–285, https://doi.org/10.1177/0309133307079055, https://doi.org/10.1177/0309133307079055, 2007.

Medlyn, B. E., Berbigier, P., Clement, R., Grelle, A., Loustau, D., Linder, S., Wingate, L., Jarvis, P. G., Sigurdsson, B. D., and McMurtrie, R. E.: Carbon balance of coniferous forests growing in contrasting climates: Model-based analysis, Agricultural and Forest Meteorology, 131, 97–124, 2005.

Meinzer, F. C.: Functional convergence in plant responses to the environment, Oecologia, 134, 1–11, 2003.

Merbold, L., Ardö, J., Arneth, A., Scholes, R. J., Nouvellon, Y., de Grandcourt, A., Archibald, S., Bonnefond, J. M., Boulain, N., Brueggemann, N., Bruemmer, C., Cappelaere, B., Ceschia, E., El-Khidir, H. a. M., El-Tahir, B. A., Falk, U., Lloyd, J., Kergoat, L., Dantec, V. L., Mougin, E., Muchinda, M., Mukelabai, M. M., Ramier, D., Roupsard, O., Timouk, F., Veenendaal, E. M., and Kutsch, W. L.: Precipitation as Driver of Carbon Fluxes in 11 African Ecosystems, Biogeosciences, 6, 1027–1041, https://doi.org/https://doi.org/10.5194/bg-6-1027-2009, 2009.

Merbold, L., Eugster, W., Stieger, J., Zahniser, M., Nelson, D., and Buchmann, N.: Greenhouse Gas Budget (CO2, CH4 and N2O) of Intensively Managed Grassland Following Restoration, Global Change Biology, 20, 1913–1928, https://doi.org/10.1111/gcb.12518, 2014.

Meyer, W. S., Kondrlova, E., and Koerber, G. R.: Evaporation of Perennial Semi-Arid Woodland in Southeastern Australia Is Adapted for Irregular but Common Dry Periods, Hydrological Processes, 29, {3714–3726}, https://doi.org/{10.1002/hyp.10467}, 2015.

Meyers, T. P. and Hollinger, S. E.: An assessment of storage terms in the surface energy balance of maize and soybean, Agricultural and Forest Meteorology, 125, 105–115, 2004.

540 Miralles, D. G., Gentine, P., Seneviratne, S. I., and Teuling, A. J.: Land–atmospheric feedbacks during droughts and heatwaves: state of the science and current challenges, Annals of the New York Academy of Sciences, 1436, 19, 2019.

Moors, E. J.: Water Use of Forests in the Netherlands, Tech. Rep. 41, Vrije Universiteit, Amsterdam, 2012.

Moureaux, C., Debacq, A., Bodson, B., Heinesch, B., and Aubinet, M.: Annual Net Ecosystem Carbon Exchange by a Sugar Beet Crop, Agricultural and Forest Meteorology, 139, 25–39, https://doi.org/https://doi.org/10.1016/j.agrformet.2006.05.009, 2006.

545 Musavi, T., Migliavacca, M., Reichstein, M., Kattge, J., Wirth, C., Black, T. A., Janssens, I., Knohl, A., Loustau, D., Roupsard, O., et al.: Stand age and species richness dampen interannual variation of ecosystem-level photosynthetic capacity, Nature ecology & evolution, 1, 0048, 2017.

Nagy, Z., Czóbel, S., Balogh, J., Horváth, L., Fóti, S., Pintér, K., Weidinger, T., Csintalan, Z., and Tuba, Z.: Some preliminary results of the Hungarian grassland ecological research: carbon cycling and greenhouse gas balances under changing, Cereal Research Communications,
550 33, 279–281, 2005.

Nardino, M., Georgiadis, T., Rossi, F., Ponti, F., Miglietta, F., and Magliulo, V.: Primary productivity and evapotranspiration of a mixed forest, in: Congress CNR-ISA Fo., Istituto per i Sistemi Agricoli e Forestali del Mediterraneo, Portici, pp. 24–25, 2002.

Nave, L. E., Gough, C. M., Maurer, K. D., Bohrer, G., Hardiman, B. S., Moine, J. L., Munoz, A. B., Nadelhoffer, K. J., Sparks, J. P., Strahm, B. D., Vogel, C. S., and Curtis, P. S.: Disturbance and the Resilience of Coupled Carbon and Nitrogen Cycling in a North Temperate
555 Forest, Journal of Geophysical Research: Biogeosciences, 116, https://doi.org/10.1029/2011JG001758, 2011.

Nelson, J. A., Pérez-Priego, O., Zhou, S., Poyatos, R., Zhang, Y., Blanken, P. D., Gimeno, T. E., Wohlfahrt, G., Desai, A. R., Gioli, B., Limousin, J.-M., Bonal, D., Paul-Limoges, E., Scott, R. L., Varlagin, A., Fuchs, K., Montagnani, L., Wolf, S., Delpierre, N., Berveiller, D., Gharun, M., Belelli Marchesini, L., Gianelle, D., Šigut, L., Mammarella, I., Siebicke, L., Andrew Black, T., Knohl, A., Hörtnagl, L., Magliulo, V., Besnard, S., Weber, U., Carvalhais, N., Migliavacca, M., Reichstein, M., and Jung, M.: Ecosystem tran-
560 spiration and evaporation: Insights from three water flux partitioning methods across FLUXNET sites, Global Change Biology, n/a, https://doi.org/10.1111/gcb.15314, https://onlinelibrary.wiley.com/doi/abs/10.1111/gcb.15314.

NOAA: National Centers for Environmental Information, State of the Climate: National Climate Report for Annual 2014, published online January 2015, retrieved on August 4, 2020 from https://www.ncdc.noaa.gov/sotc/national/201413.

Papagiannopoulou, C., Miralles, D. G., Decubber, S., Demuzere, M., Verhoest, N. E. C., Dorigo, W. A., and Waegeman, W.: A non-
565 linear Granger-causality framework to investigate climate–vegetation dynamics, Geoscientific Model Development, 10, 1945–1960, https://doi.org/10.5194/gmd-10-1945-2017, https://www.geosci-model-dev.net/10/1945/2017/, 2017.

Papale, D., Reichstein, M., Aubinet, M., Canfora, E., Bernhofer, C., Kutsch, W., Longdoz, B., Rambal, S., Valentini, R., Vesala, T., et al.: Towards a standardized processing of Net Ecosystem Exchange measured with eddy covariance technique: algorithms and uncertainty estimation, Biogeosciences, 3, 571–583, 2006.

570 Pastorello, G., Trotta, C., Canfora, E., Chu, H., Christianson, D., Cheah, Y.-W., Poindexter, C., Chen, J., Elbashandy, A., Humphrey, M., et al.: The FLUXNET2015 dataset and the ONEFlux processing pipeline for eddy covariance data, Scientific data, 7, 1–27, 2020.

Pearson, K.: On Lines and Planes of Closest Fit to Systems of Points in Space, Philosophical Magazine, 2, 559–572, 1901.

Pilegaard, K., Ibrom, A., Courtney, M. S., Hummelshøj, P., and Jensen, N. O.: Increasing Net CO2 Uptake by a Danish Beech Forest during the Period from 1996 to 2009, Agricultural and Forest Meteorology, 151, 934–946, https://doi.org/10.1016/j.agrformet.2011.02.013, 2011.

575 Potter, B. E., Teclaw, R. M., and Zasada, J. C.: The Impact of Forest Structure on Near-Ground Temperatures during Two Years of Contrasting Temperature Extremes, Agricultural and Forest Meteorology, 106, 331–336, https://doi.org/10.1016/S0168-1923(00)00220-3, 2001.

Potts, D. L., Barron-Gafford, G. A., and Scott, R. L.: Ecosystem hydrologic and metabolic flashiness are shaped by plant community traits and precipitation, Agricultural and Forest Meteorology, 279, 107 674, https://doi.org/https://doi.org/10.1016/j.agrformet.2019.107674, http://www.sciencedirect.com/science/article/pii/S0168192319302904, 2019.

580   Prescher, A.-K., Grünwald, T., and Bernhofer, C.: Land Use Regulates Carbon Budgets in Eastern Germany: From NEE to NBP, Agricultural and Forest Meteorology, 150, 1016–1025, https://doi.org/10.1016/j.agrformet.2010.03.008, 2010a.

Prescher, A.-K., Grünwald, T., and Bernhofer, C.: Land Use Regulates Carbon Budgets in Eastern Germany: From NEE to NBP, Agricultural and Forest Meteorology, 150, 1016–1025, https://doi.org/10.1016/j.agrformet.2010.03.008, 2010b.

Pryor, S. C., Barthelmie, R. J., and Jensen, B.: Nitrogen Dry Deposition at an AmeriFlux Site in a Hardwood Forest in the Midwest,
585   Geophysical Research Letters, 26, 691–694, https://doi.org/10.1029/1999GL900066, 1999.

Rambal, S., Joffre, R., Ourcival, J. M., Cavender-Bares, J., and Rocheteau, A.: The Growth Respiration Component in Eddy CO2 Flux from a Quercus Ilex Mediterranean Forest, Global Change Biology, 10, 1460–1469, https://doi.org/10.1111/j.1365-2486.2004.00819.x, 2004.

Rayment, M. B. and Jarvis, P. G.: Seasonal Gas Exchange of Black Spruce Using an Automatic Branch Bag System, Canadian Journal of Forest Research, 29, 1528–1538, https://doi.org/10.1139/x99-130, 1999a.

590   Rayment, M. B. and Jarvis, P. G.: Seasonal Gas Exchange of Black Spruce Using an Automatic Branch Bag System, Canadian Journal of Forest Research, 29, 1528–1538, https://doi.org/10.1139/x99-130, 1999b.

Reich, P. B., Walters, M. B., Ellsworth, D. S., Vose, J. M., Volin, J. C., Gresham, C., and Bowman, W. D.: Relationships of Leaf Dark Respiration to Leaf Nitrogen, Specific Leaf Area and Leaf Life-Span: A Test across Biomes and Functional Groups, Oecologia, 114, 471–482, https://doi.org/10.1007/s004420050471, 1998.

595   Reichstein, M., Tenhunen, J. D., Roupsard, O., Ourcival, J.-m., Rambal, S., Miglietta, F., Peressotti, A., Pecchiari, M., Tirone, G., and Valentini, R.: Severe drought effects on ecosystem CO2 and H2O fluxes at three Mediterranean evergreen sites: revision of current hypotheses?, Global Change Biology, 8, 999–1017, 2002.

Reichstein, M., Falge, E., Baldocchi, D., Papale, D., Aubinet, M., Berbigier, P., Bernhofer, C., Buchmann, N., Gilmanov, T., Granier, A., Grünwald, T., Havránková, K., Ilvesniemi, H., Janous, D., Knohl, A., Laurila, T., Lohila, A., Loustau, D., Matteucci, G., Meyers, T.,
600   Miglietta, F., Ourcival, J.-M., Pumpanen, J., Rambal, S., Rotenberg, E., Sanz, M., Tenhunen, J., Seufert, G., Vaccari, F., Vesala, T., Yakir, D., and Valentini, R.: On the separation of net ecosystem exchange into assimilation and ecosystem respiration: review and improved algorithm, Global Change Biology, 11, 1424–1439, https://doi.org/10.1111/j.1365-2486.2005.001002.x, https://onlinelibrary.wiley.com/doi/abs/10.1111/j.1365-2486.2005.001002.x, 2005.

Rey, A., Pegoraro, E., Tedeschi, V., Parri, I. D., Jarvis, P. G., and Valentini, R.: Annual Variation in Soil Respiration and Its Components in a
605   Coppice Oak Forest in Central Italy, Global Change Biology, 8, 851–866, https://doi.org/10.1046/j.1365-2486.2002.00521.x, 2002.

Reynolds, J. F., Kemp, P. R., Ogle, K., and Fernández, R. J.: Modifying the 'pulse–reserve' paradigm for deserts of North America: precipitation pulses, soil water, and plant responses, Oecologia, 141, 194–210, 2004.

Rodrigues, A., Pita, G., Mateus, J., Kurz-Besson, C., Casquilho, M., Cerasoli, S., Gomes, A., and Pereira, J.: Eight years of continuous carbon fluxes measurements in a Portuguese eucalypt stand under two main events: Drought and felling, Agricultural and Forest Meteorology,
610   151, 493–507, 2011.

Rothstein, D. E., Zak, D. R., Pregitzer, K. S., and Curtis, P. S.: Kinetics of Nitrogen Uptake by Populus Tremuloides in Relation to Atmospheric CO2 and Soil Nitrogen Availability, Tree Physiology, 20, 265–270, https://doi.org/10.1093/treephys/20.4.265, 2000.

Ruehr, N. K., Martin, J. G., and Law, B. E.: Effects of Water Availability on Carbon and Water Exchange in a Young Ponderosa Pine Forest: Above- and Belowground Responses, Agricultural and Forest Meteorology, 164, 136–148,
615   https://doi.org/10.1016/j.agrformet.2012.05.015, 2012a.

Ruehr, N. K., Martin, J. G., and Law, B. E.: Effects of Water Availability on Carbon and Water Exchange in a Young Ponderosa Pine Forest: Above- and Belowground Responses, Agricultural and Forest Meteorology, 164, 136–148, https://doi.org/10.1016/j.agrformet.2012.05.015, 2012b.

Ruehr, N. K., Martin, J. G., and Law, B. E.: Effects of Water Availability on Carbon and Water Exchange in a
620   Young Ponderosa Pine Forest: Above- and Belowground Responses, Agricultural and Forest Meteorology, 164, 136–148, https://doi.org/10.1016/j.agrformet.2012.05.015, 2012c.

Ruehr, N. K., Martin, J. G., and Law, B. E.: Effects of Water Availability on Carbon and Water Exchange in a Young Ponderosa Pine Forest: Above- and Belowground Responses, Agricultural and Forest Meteorology, 164, 136–148, https://doi.org/10.1016/j.agrformet.2012.05.015, 2012d.

625   Ruehr, N. K., Martin, J. G., and Law, B. E.: Effects of Water Availability on Carbon and Water Exchange in a Young Ponderosa Pine Forest: Above- and Belowground Responses, Agricultural and Forest Meteorology, 164, 136–148, https://doi.org/10.1016/j.agrformet.2012.05.015, 2012e.

Runge, J., Bathiany, S., Bollt, E., Camps-Valls, G., Coumou, D., Deyle, E., Glymour, C., Kretschmer, M., Mahecha, M. D., Muñoz-Marí, J., et al.: Inferring causation from time series in Earth system sciences, Nature communications, 10, 2553, 2019a.

630   Runge, J., Nowack, P., Kretschmer, M., Flaxman, S., and Sejdinovic, D.: Detecting and quantifying causal associations in large nonlinear time series datasets, Science Advances, 5, 2019b.

Sagerfors, J., Lindroth, A., Grelle, A., Klemedtsson, L., Weslien, P., and Nilsson, M.: Annual CO_2 exchange between a nutrient-poor, minerotrophic, boreal mire and the atmosphere, Journal of Geophysical Research: Biogeosciences, 113, https://doi.org/10.1029/2006JG000306, https://agupubs.onlinelibrary.wiley.com/doi/abs/10.1029/2006JG000306, 2008.

635   Saleska, S. R., Miller, S. D., Matross, D. M., Goulden, M. L., Wofsy, S. C., da Rocha, H. R., de Camargo, P. B., Crill, P., Daube, B. C., de Freitas, H. C., Hutyra, L., Keller, M., Kirchhoff, V., Menton, M., Munger, J. W., Pyle, E. H., Rice, A. H., and Silva, H.: Carbon in Amazon Forests: Unexpected Seasonal Fluxes and Disturbance-Induced Losses, Science, 302, 1554–1557, https://doi.org/10.1126/science.1091165, 2003.

Sanz, M., Carrara, A., Gimeno, C., Bucher, A., and Lopez, R.: Effects of a dry and warm summer conditions on CO_2 and energy fluxes from
640   three Mediterranean ecosystems, in: Geophys. Res. Abstr, vol. 6, p. 3239, 2004.

Schade, G. W., Goldstein, A. H., and Lamanna, M. S.: Are Monoterpene Emissions Influenced by Humidity?, Geophysical Research Letters, 26, 2187–2190, https://doi.org/10.1029/1999GL900444.

Schreiber, T.: Measuring Information Transfer, Phys. Rev. Lett., 85, 461–464, https://doi.org/10.1103/PhysRevLett.85.461, https://link.aps.org/doi/10.1103/PhysRevLett.85.461, 2000.

645   Schuldt, B., Buras, A., Arend, M., Vitasse, Y., Beierkuhnlein, C., Damm, A., Gharun, M., Grams, T. E., Hauck, M., Hajek, P., Hartmann, H., Hiltbrunner, E., Hoch, G., Holloway-Phillips, M., Körner, C., Larysch, E., Lübbe, T., Nelson, D. B., Rammig, A., Rigling, A., Rose, L., Ruehr, N. K., Schumann, K., Weiser, F., Werner, C., Wohlgemuth, T., Zang, C. S., and Kahmen, A.: A first assessment of the impact of the extreme 2018 summer drought on Central European forests, Basic and Applied Ecology, 45, 86 – 103, https://doi.org/https://doi.org/10.1016/j.baae.2020.04.003, http://www.sciencedirect.com/science/article/pii/S1439179120300414, 2020.

650 Schwalm, C. R., Anderegg, W. R., Michalak, A. M., Fisher, J. B., Biondi, F., Koch, G., Litvak, M., Ogle, K., Shaw, J. D., Wolf, A., et al.: Global patterns of drought recovery, Nature, 548, 202–205, 2017.

Scott, R. L., Huxman, T. E., Cable, W. L., and Emmerich, W. E.: Partitioning of Evapotranspiration and Its Relation to Carbon Dioxide Exchange in a Chihuahuan Desert Shrubland, Hydrological Processes, 20, 3227–3243, https://doi.org/10.1002/hyp.6329, 2006.

Scott, R. L., Cable, W. L., and Hultine, K. R.: The Ecohydrologic Significance of Hydraulic Redistribution in a Semiarid Savanna, Water
655   Resources Research, 44, https://doi.org/10.1029/2007WR006149, 2008.

Shaver, G. R., Street, L. E., Rastetter, E. B., Van Wijk, M. T., and Williams, M.: Functional convergence in regulation of net CO2 flux in heterogeneous tundra landscapes in Alaska and Sweden, Journal of Ecology, 95, 802–817, https://doi.org/10.1111/j.1365-2745.2007.01259.x, https://besjournals.onlinelibrary.wiley.com/doi/abs/10.1111/j.1365-2745.2007.01259.x, 2007.

Sippel, S., Forkel, M., Rammig, A., Thonicke, K., Flach, M., Heimann, M., Otto, F. E. L., Reichstein, M., and Mahecha, M. D.: Contrasting
660   and interacting changes in simulated spring and summer carbon cycle extremes in European ecosystems, Environmental Research Letters, 12, 075 006, https://doi.org/10.1088/1748-9326/aa7398, https://doi.org/10.1088%2F1748-9326%2Faa7398, 2017.

Sippel, S., Reichstein, M., Ma, X., Mahecha, M. D., Lange, H., Flach, M., and Frank, D.: Drought, heat, and the carbon cycle: a review, Current Climate Change Reports, 4, 266–286, 2018.

Spirtes, P. and Glymour, C.: An Algorithm for Fast Recovery of Sparse Causal Graphs, Social Science Computer Review, 9, 62–72,
665   https://doi.org/10.1177/089443939100900106, https://doi.org/10.1177/089443939100900106, 1991.

Sugihara, G., May, R., Ye, H., Hsieh, C.-h., Deyle, E., Fogarty, M., and Munch, S.: Detecting Causality in Complex Ecosystems, Science, 338, 496–500, https://doi.org/10.1126/science.1227079, http://science.sciencemag.org/content/338/6106/496, 2012.

Suni, T., Rinne, J., Reissell, A., Altimir, N., Keronen, P., Rannik, U., Dal Maso, M., Kulmala, M., and Vesala, T.: Long-Term Measurements of Surface Fluxes above a Scots Pine Forest in Hyytiala, Southern Finland, 1996-2001, BOREAL ENVIRONMENT RESEARCH, 8,
670   {287–301}, 2003.

Székely, G. J., Rizzo, M. L., and Bakirov, N. K.: Measuring and testing dependence by correlation of distances, Ann. Statist., 35, 2769–2794, https://doi.org/10.1214/009053607000000505, https://doi.org/10.1214/009053607000000505, 2007.

Tamrakar, R., Rayment, M. B., Moyano, F., Mund, M., and Knohl, A.: Implications of structural diversity for seasonal and annual carbon dioxide fluxes in two temperate deciduous forests, Agricultural and Forest Meteorology, 263, 465 – 476,
675   https://doi.org/https://doi.org/10.1016/j.agrformet.2018.08.027, http://www.sciencedirect.com/science/article/pii/S0168192318302934, 2018.

Tang, J., Baldocchi, D. D., Qi, Y., and Xu, L.: Assessing Soil CO2 Efflux Using Continuous Measurements of CO2 Profiles in Soils with Small Solid-State Sensors, Agricultural and Forest Meteorology, 118, 207–220, https://doi.org/10.1016/S0168-1923(03)00112-6, 2003.

Tedeschi, V., Rey, A., Manca, G., Valentini, R., Jarvis, P. G., and Borghetti, M.: Soil respiration in a Mediterranean oak forest at different
680   developmental stages after coppicing, Global Change Biology, 12, 110–121, 2006.

Thomas, S. C., Halpern, C. B., Falk, D. A., Liguori, D. A., and Austin, K. A.: Plant diversity in managed forests: understory responses to thinning and fertilization, Ecological applications, 9, 864–879, 1999a.

Thomas, S. C., Halpern, C. B., Falk, D. A., Liguori, D. A., and Austin, K. A.: Plant diversity in managed forests: understory responses to thinning and fertilization, Ecological applications, 9, 864–879, 1999b.

685 Thomas, S. C., Halpern, C. B., Falk, D. A., Liguori, D. A., and Austin, K. A.: Plant diversity in managed forests: understory responses to thinning and fertilization, Ecological applications, 9, 864–879, 1999c.

Thum, T., Aalto, T., Laurila, T., Aurela, M., Kolari, P., and Hari, P.: Parametrization of Two Photosynthesis Models at the Canopy Scale in a Northern Boreal Scots Pine Forest, Tellus B, 59, 874–890, https://doi.org/10.1111/j.1600-0889.2007.00305.x, 2007.

690 Valentini, R., Angelis, P. D., Matteucci, G., Monaco, R., Dore, S., and Mucnozza, G. E. S.: Seasonal Net Carbon Dioxide Exchange of a Beech Forest with the Atmosphere, Global Change Biology, 2, 199–207, https://doi.org/10.1111/j.1365-2486.1996.tb00072.x, 1996.

Valentini, R., Matteucci, G., Dolman, A., Schulze, E.-D., Rebmann, C., Moors, E., Granier, A., Gross, P., Jensen, N., Pilegaard, K., et al.: Respiration as the main determinant of carbon balance in European forests, Nature, 404, 861–865, 2000.

van der Molen, M. K., van Huissteden, J., Parmentier, F. J. W., Petrescu, A. M. R., Dolman, A. J., Maximov, T. C., Kononov, A. V., Karsanaev, S. V., and Suzdalov, D. A.: The Growing Season Greenhouse Gas Balance of a Continental Tundra Site in the Indigirka Lowlands, NE

695 Siberia, Biogeosciences, 4, 985–1003, https://doi.org/https://doi.org/10.5194/bg-4-985-2007, 2007.

Vitale, L., Di Tommasi, P., D'Urso, G., and Magliulo, V.: The Response of Ecosystem Carbon Fluxes to LAI and Environmental Drivers in a Maize Crop Grown in Two Contrasting Seasons, International Journal of Biometeorology, 60, 411–420, https://doi.org/10.1007/s00484-015-1038-2, 2016.

von Buttlar, J., Zscheischler, J., Rammig, A., Sippel, S., Reichstein, M., Knohl, A., Jung, M., Menzer, O., Arain, M. A., Buchmann, N.,

700 Cescatti, A., Gianelle, D., Kiely, G., Law, B. E., Magliulo, V., Margolis, H., McCaughey, H., Merbold, L., Migliavacca, M., Montagnani, L., Oechel, W., Pavelka, M., Peichl, M., Rambal, S., Raschi, A., Scott, R. L., Vaccari, F. P., van Gorsel, E., Varlagin, A., Wohlfahrt, G., and Mahecha, M. D.: Impacts of droughts and extreme-temperature events on gross primary production and ecosystem respiration: a systematic assessment across ecosystems and climate zones, Biogeosciences, 15, 1293–1318, https://doi.org/10.5194/bg-15-1293-2018, https://www.biogeosciences.net/15/1293/2018/, 2018.

705 Wagg, C., O'Brien, M. J., Vogel, A., Scherer-Lorenzen, M., Eisenhauer, N., Schmid, B., and Weigelt, A.: Plant diversity maintains long-term ecosystem productivity under frequent drought by increasing short-term variation, Ecology, 98, 2952–2961, https://doi.org/10.1002/ecy.2003, https://esajournals.onlinelibrary.wiley.com/doi/abs/10.1002/ecy.2003, 2017.

Wales, S. B., Kreider, M. R., Atkins, J., Hulshof, C. M., Fahey, R. T., Nave, L. E., Nadelhoffer, K. J., and Gough, C. M.: Stand age, disturbance history and the temporal stability of forest production, Forest Ecology and Management, 460, 117 865,

710 https://doi.org/https://doi.org/10.1016/j.foreco.2020.117865, http://www.sciencedirect.com/science/article/pii/S0378112719315191, 2020.

Wang, C., Bond-Lamberty, B., and Gower, S. T.: Environmental Controls on Carbon Dioxide Flux from Black Spruce Coarse Woody Debris, Oecologia, 132, 374–381, https://doi.org/10.1007/s00442-002-0987-4, 2002a.

Wang, C., Bond-Lamberty, B., and Gower, S. T.: Environmental Controls on Carbon Dioxide Flux from Black Spruce Coarse Woody Debris,

715 Oecologia, 132, 374–381, https://doi.org/10.1007/s00442-002-0987-4, 2002b.

Wang, C., Bond-Lamberty, B., and Gower, S. T.: Environmental Controls on Carbon Dioxide Flux from Black Spruce Coarse Woody Debris, Oecologia, 132, 374–381, https://doi.org/10.1007/s00442-002-0987-4, 2002c.

Westergaard-Nielsen, A., Lund, M., Hansen, B. U., and Tamstorf, M. P.: Camera Derived Vegetation Greenness Index as Proxy for Gross Primary Production in a Low Arctic Wetland Area, ISPRS Journal of Photogrammetry and Remote Sensing, 86, 89–99,

720 https://doi.org/10.1016/j.isprsjprs.2013.09.006, 2013.

Wofsy, S. C., Goulden, M. L., Munger, J. W., Fan, S.-M., Bakwin, P. S., Daube, B. C., Bassow, S. L., and Bazzaz, F. A.: Net Exchange of CO2 in a Mid-Latitude Forest, Science, 260, 1314–1317, https://doi.org/10.1126/science.260.5112.1314, 1993.

Wohlfahrt, G., Hammerle, A., Haslwanter, A., Bahn, M., Tappeiner, U., and Cernusca, A.: Seasonal and inter-annual variability of the net ecosystem CO2 exchange of a temperate mountain grassland: Effects of weather and management, Journal of Geophysical Research: Atmospheres, 113, 2008.

725

Xu, L., Baldocchi, D. D., and Tang, J.: How Soil Moisture, Rain Pulses, and Growth Alter the Response of Ecosystem Respiration to Temperature, Global Biogeochemical Cycles, 18, https://doi.org/10.1029/2004GB002281, 2004.

Yi, C., Davis, K. J., Berger, B. W., and Bakwin, P. S.: Long-Term Observations of the Dynamics of the Continental Planetary Boundary Layer, Journal of the Atmospheric Sciences, 58, 1288–1299, https://doi.org/10.1175/1520-0469(2001)058<1288:LTOOTD>2.0.CO;2, 2001.

730

Zeller, K. and Hehn, T.: Measurements of Upward Turbulent Ozone Fluxes above a Subalpine Spruce-Fir Forest, Geophysical Research Letters, 23, 841–844, 1996.

Zeller, K. F. and Nikolov, N. T.: Quantifying Simultaneous Fluxes of Ozone, Carbon Dioxide and Water Vapor above a Subalpine Forest Ecosystem, Environmental Pollution, 107, 1–20, https://doi.org/10.1016/S0269-7491(99)00156-6, 2000.

Zielis, S., Etzold, S., Zweifel, R., Eugster, W., Haeni, M., and Buchmann, N.: NEP of a Swiss Subalpine Forest Is Significantly Driven

735

Not Only by Current but Also by Previous Year's Weather, Biogeosciences, 11, 1627–1635, https://doi.org/https://doi.org/10.5194/bg-11-1627-2014, 2014.

Zscheischler, J., Martius, O., Westra, S., Bevacqua, E., Raymond, C., Horton, R. M., van den Hurk, B., AghaKouchak, A., Jézéquel, A., Mahecha, M. D., et al.: A typology of compound weather and climate events, Nature reviews earth & environment, pp. 1–15, 2020.